European Rail Research Institute

ERRI D 170/DT 283

RESPONSE OF THE RAILWAY TRACK UNDER EXTERNAL LOADING

Stresses in a fastening system caused by wheel forces

by Josef Turek (ČD)
Edited by Mr A. Kamiński (ERRI)

UTRECHT, September 1994

ERRI D 170/DT 283

RESPONSE OF THE RAILWAY TRACK UNDER EXTERNAL LOADING

Stresses in a fastening system caused by wheel forces

by Josef Turek (ČD)
Edited by Mr A. Kamiński (ERRI)

UTRECHT, September 1994

Report No.: ERRI D 170/DT 283	Type of report: Technical Document	Date: 1994-9-30

Title and Subtitle:

Response of the railway track under external loading
Stresses in a fastening system caused by wheel forces

Supplementary Notes:

English
French
German

Author(s): Josef Turek (ČD)
Edited by Mr A. Kamiński (ERRI)

No. of incl. Pages: 53
Figures: 34
Tables: 8

Classification:

Performing Body: European Rail Research Institute (ERRI)
Arthur van Schendelstraat 754
NL - 3511 MK UTRECHT

Price:
Hfl. 160,-

Sponsoring Body: UIC SC 7G
16, rue Jean Rey
F - 75015 Paris, France

Fee for right of use:
Hfl. 350,-

Summary:

A railway track model is presented in order to describe the influence of the non-linear behaviour of the various elements of the fastening system on the forces and deformations affecting the fastening system.

Availability of the report: Unrestricted	Date: 1994-9-30	Approved Performing Body:	Date:
Keywords: Track, fastening systems, non-linear modelling		Approved Sponsoring Body: Not applicable	Date: N/A

DEFINITION OF VARIABLES

VPE Vertical displacement of outside of rail foot [mm]

VPI Vertical displacement of inside of rail foot [mm]

RC Angle of rotation of rail head [°]

RP Angle of rotation of rail foot [°]

HP Horizontal displacement of rail foot [mm]

HC Horizontal displacement of rail head [mm]

RELATED DOCUMENTS

Statutory texts cited	Other documents
	ERRI D 170/RP 5 ERRI D 170/DT 282 ERRI D 170/DT 285 ERRI D 170/DT 302 ERRI D 170/DT 303 ERRI D 170/DT 304

The values of the function F(Δ) for $\Delta > \Delta_{np}$ are given by the line determined by points $[\Delta_{np-1}; F(\Delta_{np-1})]$ and $[\Delta_{np}; F(\Delta_{np})]$. For negative Δ values $F(\Delta) = 0$ applies. Account is thus taken of the fact that the pad cannot produce tensile stresses. The function F(Δ) is described by the following:

$$F(\Delta) = \begin{cases} 0 \text{ for } \Delta < 0 \\ F(\Delta) \text{ for } 0 \le \Delta \le \Delta_{np} \text{ cubic spline} \\ \dfrac{1}{\Delta_{np} - \Delta_{np-1}} [(F_{np} - F_{np-1}) \cdot \Delta + \Delta_{np} \cdot F_{np-1} - \Delta_{np-1} \cdot F_{np}] \text{ for } \Delta > \Delta_{np} \end{cases} \quad (1)$$

1.2.2 Clip

The stress-strain diagram of one clip is assumed to be in the same form as the diagram of the pad (see Fig. 2 [p. 13]). Again, preloading of the clip is not assumed. The stress-strain diagram is described by the following function $F_c(\Delta_c)$:

$$F_c(\Delta_c) = \begin{cases} 0 \text{ for } \Delta_c < 0 \\ F_c(\Delta_c) \text{ for } 0 \le \Delta_c \le \Delta_{c_{np}} \text{ cubic spline} \\ \dfrac{1}{\Delta_{c_{np}} - \Delta_{c_{np-1}}} [(F_{c_{np}} - F_{c_{np-1}}) \Delta_c + \Delta_{c_{np}} F_{c_{np-1}} - \Delta_{c_{np-1}} F_{c_{np}}] \text{ for } \Delta_c > \Delta_{c_{np}} \end{cases} \quad (2)$$

The stress-strain diagrams used for the various clips are given in Fig. 5 [p. 16].

Again, pre-loading of the clip is not assumed. The stress-strain diagram is described by the breaking (turning) point $[\Delta_{c1}; F_{c1}]$ and by the gradient of the second line, element k_c. The function $F_c(\Delta_c)$ is described by the following:

$$F_c(\Delta_c) = \begin{cases} \dfrac{F_{c1}}{\Delta_{c1}} \cdot \Delta_c \text{ for } \Delta_c \le \Delta_{c1} \\ k_c \cdot (\Delta_c - \Delta_{c1}) + F_{c1} \text{ for } \Delta_c > \Delta_{c1} \end{cases} \quad (3)$$

1.2.3 Lateral stiffness

The lateral stiffness of the whole fastening system is replaced by one spring, fixing the rail foot in the lateral direction. The stress-strain diagram of this spring is bilinear and antimetric (Fig. 6 [p. 17]).

The function $F_H(\Delta_H)$ is described by the following:

$$F_H(\Delta_H) = \begin{cases} \dfrac{F_{H1}}{\Delta_{H1}} \cdot \Delta_H \text{ for } 0 \le \Delta_H \le \Delta_{H1} \\ k_H \cdot (\Delta_H - \Delta_{H1}) + F_{H1} \text{ for } \Delta_H > \Delta_{H1} \\ -F_H(\Delta_H) \text{ for } \Delta_H < 0 \end{cases} \quad (4)$$

1.2.4 Initial state of the fastening system

The initial state of the fastening system is assumed to be the assembled state without external loading. This means that both clips have half of the toe load $T_L/2$. This force deforms the clip on value Δ_{co}, for which the following equation applies:

$$\frac{1}{2} \cdot T_L = F_c(\Delta_{co}) \quad (5)$$

The pad is deformed on constant value Δ_o, for which the following equation applies:

$$T_L = F(\Delta_o) \quad (6)$$

The relative vertical deflection between the rail foot centre and sleeper v_z, the horizontal deflection v_y, and torsion of the rail foot centre to sleeper v_φ are defined from the initial state. For subsequent purposes we note the rigid body motion of the rail foot as function $g(\xi)$:

$$g(\xi) = v_z + v_\varphi \cdot \xi \quad (7)$$

1.2.5 Relations between forces and deformations in the fastening system

In the fastening system, the following forces arise (Fig. 7 [p. 18]):

- horizontal force X_y
- vertical force X_z
- moment X_φ.

The following equations define the relations between these forces and deformations if we assume only rigid body motion of the rail foot $g(\xi)$:

$$\begin{aligned} X_y &= X_y(v_y) = F_H(v_y) \\ X_z &= X_z(v_z, v_\varphi) = \frac{1}{d} \int_{-\frac{d}{2}}^{\frac{d}{2}} F(g(\xi) + \Delta_0) d\xi - F_c(\Delta_{co} - g(\tfrac{d_c}{2})) - F_c(\Delta_{co} - g(-\tfrac{d_c}{2})) \\ X_\varphi &= X_\varphi(v_z, v_\varphi) = \frac{1}{d} \int_{-\frac{d}{2}}^{\frac{d}{2}} F(g(\xi) + \Delta_0)\, \xi\, d\xi - F_c(\Delta_{co} - g(\tfrac{d_c}{2}))\frac{d_c}{2} - F_c(\Delta_{co} - g(-\tfrac{d_c}{2}))\frac{d_c}{2} \end{aligned} \quad (8)$$

The rail foot is not deformed only as a rigid body but has its own deformation caused by pad reaction and the forces in the clips. Via a folded plate program it was found that this complementary foot deformation was of a local nature only and that it decreased almost to zero over a distance of about 15 cm. In other words, local deformations of the foot do not influence each other. This made it possible to set down Equation (8) not only for rigid body motion, but also for any local deformation of the foot. The geometric relations are shown in Fig. 8 [p. 19].

The following equation is valid for the unknown function v(ξ):

$$g(\xi) - \frac{1}{d}\int_{-\frac{d}{2}}^{\frac{d}{2}} G(\xi, \eta) \cdot F(v(\eta) + \Delta_0)\, d\eta = v(\xi) \qquad (9)$$

where:

g(ξ) - rigid body motion of the rail foot

ξ,η - auxiliary coordinates

v(ξ) - full foot deformation sought

G(ξ,η) - G(η,ξ) - Green's function, influence line of local foot deformation. This function is computed by the folded plate method in twelve discrete points of the coordinates ξ, η. Therefore function G takes the form of a 12 x 12 matrix.

Equation (9) is known as Fredholm's integral equation, which can always be solved according to Banach's theorem of fixed points, because the operator of this equation is convergent. Unfortunately, the convergence speed of this method is much lower than that of the Newton-Raphson method (discussed later). In order to reach an accuracy of about $1e^{-6}$ [m] we usually had to use about 15 cycles of the iteration.

Now we can correct Equations (8) in order to consider the local foot deformation v(ξ). In this case, the Equations (8) have exactly the same form, only we use v(ξ) instead of g(ξ). Such corrected equations take the form of vectors:

$$\vec{X} = \vec{X}(\vec{v}) \qquad (10)$$
$$\text{where } \vec{X} = \{X_y, X_z, X_\varphi\},\ \vec{v} = \{v_y, v_z, v_\varphi\}$$

Equation (10) enables unknown forces to be computed, if the deformations are known. For the model of the track, the "static method" is used to compute deformations where the forces are known. Inversion relations to the equation (9) are therefore needed:

$$\vec{v} = \vec{v}(\vec{X}) \qquad (11)$$

This means that we have to find the root of the following equation

$$\vec{X}(\vec{v}) - \vec{X}_o = \vec{O} \qquad (12)$$

where $\vec{X}_O$ is a vector of the known forces. This operation is carried out by the Newton-Raphson method, discussed later in detail.

1.3 *Sleeper model*

The influence of the sleeper is replaced by a vertical spring with spring constant k_{sz} = 89.2 MN/m and by a torsion spring with torsion spring constant $k_{s\varphi}$ = 8.846 MNm/rad. In this way we obtain the entire deflection of the rail:

$$\vec{u} = \vec{u}(\vec{X}) = \vec{v}(\vec{X}) + \left\{0, \frac{X_z}{k_{sz}}, \frac{X_\varphi}{k_{s\varphi}}\right\}^T \qquad (13)$$

Using the deflection of a point of the sleeper under the rail (rail seat) as a basis, calculations can be carried out to establish the relative deflection of rail and sleeper.

1.4 *Description of the track model*

The static method was chosen as the basic method for a non-linear solution. The primary system is created by the simply supported UIC 60 beam with a span of 13 m. This simple beam is analysed by the folded plate method. The cross section of the UIC 60 rail is replaced by a folded plate cross section as shown in Fig. 9 [p. 20]. The influence of the sleeper with index i is replaced by the unknown forces X_{y1}, X_{z1}, $X_{\varphi 1}$.

Because the structure is symmetrical, we obtain n = 8 sleepers and their influence is replaced by 24 unknown force - variables. The unknown forces are expressed as vectors:

$$\vec{X} = \begin{Bmatrix} \{\vec{X}_y\} \\ \{\vec{X}_z\} \\ \{\vec{X}_\varphi\} \end{Bmatrix} \qquad (14)$$

where:
and so on.

The corresponding foot centre replacement is described by the vector:

$$\{\vec{X}_y\} = \begin{Bmatrix} X_{y0} \\ X_{y1} \\ \cdot \\ \cdot \\ \cdot \\ X_{y7} \end{Bmatrix} \tag{15}$$

$$\vec{u} = \begin{Bmatrix} \{\vec{u}_y\} \\ \{\vec{u}_z\} \\ \{\vec{u}_\varphi\} \end{Bmatrix} \tag{16}$$

For the corresponding elements of the vectors $\vec{X}$ and $\vec{u}$, Equations (10), (11) and (13) apply. Thus we can write:

$$\vec{X} = \vec{X}(\vec{u}) \tag{17}$$

$$\vec{u} = \vec{u}(\vec{X}) \tag{18}$$

The system of non-linear equations of the static method can be expressed as:

$$[\delta]\ \vec{X} + \vec{\delta}_p = \vec{u}(\vec{X}) \tag{19}$$

where matrix $[\delta]_{24,24}$ is the matrix representing compliance of the primary system. Vector $\vec{\delta}$ is created from the value of the vector $\vec{u}$ for the primary system loaded with forces H, Y, Q and e. The symmetric matrix $[\delta]_{24,24}$ has the following structure:

$$[\delta] = \begin{bmatrix} [\delta_{yy}] & [0] & [\delta_{y\varphi}] \\ [0] & [\delta_{zz}] & [0] \\ [\delta_{\varphi y}] & [0] & [\delta_{\varphi\varphi}] \end{bmatrix} \tag{20}$$

The elements of the matrix $[\delta]_{24,24}$ and vector $\vec{\delta}_p$ are computed using a commercial program based on the folded plate method [see Bibliography].

The basic problem of the track model described is to solve Equation (19). The standard method based on Banach's theorem about a fixed point failed. The Newton-Raphson method was therefore used. The system of Equations (19) is reformulated as follows:

$$[\delta]\ \vec{X} + \vec{\delta}_p - \vec{u}(\vec{X}) = \vec{O} \tag{21}$$

expressed in symbols:

$$B\vec{X} = \vec{O} \tag{22}$$

According to Newton-Raphson's method, the following sequence of vectors $\{\vec{X}^k\}$ is convergent to the root of Equation (19):

$$\vec{X}^{k+1} = \vec{X}^k - [J(\vec{X}^k)]^{-1} \cdot B\vec{X}^k \tag{23}$$

For numerical computation the following form of Equation (23) is more suitable:

$$[J(\vec{X}^k)]\ \vec{X}^{k+1} = [J(\vec{X}^k)]\ \vec{X}^k - B\vec{X}^k \tag{24}$$

where matrix

$$[J(\vec{X})] = \frac{\partial B\vec{X}}{\partial \vec{X}} = [\delta] - \frac{\partial \vec{u}(\vec{X})}{\partial \vec{X}} \tag{25}$$

known as Jacobi's matrix has the following structure:

$$\left[\frac{\partial \vec{u}(\vec{X})}{\partial \vec{X}}\right] = \begin{bmatrix} \left[\frac{\partial \vec{u}_y}{\partial \vec{X}_y}\right] & [0] & [0] \\ [0] & \left[\frac{\partial \vec{u}_z}{\partial \vec{X}_z}\right] & \left[\frac{\partial \vec{u}_z}{\partial \vec{X}_\varphi}\right] \\ [0] & \left[\frac{\partial \vec{u}_\varphi}{\partial \vec{X}_z}\right] & \left[\frac{\partial \vec{u}_\varphi}{\partial \vec{X}_\varphi}\right] \end{bmatrix} \tag{26}$$

For the first approximation of vector $\vec{X}$ in Equation (24) a linear solution of the problem is used. The accuracy of Equation (19) was chosen to be $1e^{-7}$ m and $1e^{-6}$ rad (the difference between the left and right side of Equation (19) has to be less than these values). This accuracy was usually reached in three to five iterations.

2 NON-LINEAR RESULTS

2.1 *Input data*

Using the non-linear program, six loading cases described in Technical Document ERRI D 170/DT 276 were computed for fastening systems using seven different pads (see also Technical Document ERRI D 170/DT 302):

Pandrol, tested by SNCF
Pandrol, tested by BR
ZW 700, tested by SNCF
SNCF 9 mm, tested by SNCF
SNCF 4.5 mm, tested by SNCF
ZW 687a, tested by SNCF
ZW 687a, tested by DB/DR.

See Figs 3 and 4 [p. 14 and 15] for the stress-strain diagram of the pads.

The following three clips were used:

Pandrol,
Skl 14,
Nabla.

See Fig. 5 [p. 16] for the stress-strain diagram of one clip.

Input data for linear and non-linear computations are given in Tab. 1 [p. 46].

The variables in Tab. 1 [p. 46] are defined as follows: $K_{pad,lin}$ is the linearized pad vertical stiffness, for which the following equation applies:

$$k_{pad,lin} = \frac{60\,[kN]}{F^{-1}\,(Toe\ Load + 60) - F^{-1}\,(Toe\ Load)} \qquad \textbf{(27)}$$

where:

F: stress-strain diagram of the pad (Figs 3 and 4 [p. 14 and 15]).

k_{lin} is the linearized vertical stiffness of the fastening system, for which the following equation applies:

$$k_{lin} = k_{pad,lin} + 2\,\frac{ToeLoad/2}{F_c^{-1}\,(ToeLoad/2)} \qquad \textbf{(28)}$$

where:

F: stress-strain diagram of the clip (Fig. 5 [p. 16])

The linear torsion stiffness k_φ of the fastening system is derived for k_{lin} by:

$$k_\varphi = \frac{1}{12}\,k_{lin} \cdot d^2 \qquad \textbf{(29)}$$

where d is pad width.

The variable: k_{lat} is the linear lateral stiffness of the fastening system used.

The space graph of rail foot local deformation is shown in Fig. 10 [p. 21]. This graph represents the situation of the fixed rail foot centre. The external unit loading (1 MN) applies at the edge of the rail foot.

2.2 *Linear and non-linear model results*

The non-linear model of the track is described by Equation (19). The first approximation of the unknown force vector {X} is given by the linear model result, for which the following equation applies:

$$[\delta]\,\vec{X} + \vec{\delta}_p = \begin{Bmatrix} k_{lat} \cdot \{\vec{X}_y\} \\ k_{lin} \cdot \{\vec{X}_z\} \\ k_\varphi \cdot \{\vec{X}_\varphi\} \end{Bmatrix} \qquad \textbf{(30)}$$

Equation (30) is a system of ordinary linear algebraic equations solvable by the usual methods.

Figs. 11 and 12 [p. 22 and 23] show graphs of the "contact zone" for different fastening systems, derived from Tab. 1 [p. 46]. The contact zone is defined as the area in plane X_z, X_φ (vertical force and moment applied to pad) where for any combination of X_z and X_φ the gap

between rail foot and pad does not arise. The dashed lines are valid for linear behaviour of the pads and for a 25 kN toe load (the border between a contact and gap zone does not depend on stiffness in the linear case).

Figs. 13 - 20 [p. 24 - 31] show the model simulation results of the SNCF laboratory inclined tests. Only the Nabla clip is used for this simulation. The solid curves express the test results and dotted curves are simulated by the non-linear "small" model (covering with one fastening system). The symbol VE (VI) means relative vertical deflection of the external (internal) edge of the rail foot. The bending moment in the fastening system is related to external test load as follow:

$$X_\varphi = Y * 0.16 - Q * 0.042 \ [MNm]$$
$$Y = F \cdot \sin\alpha \qquad \textbf{(31)}$$
$$Q = F \cdot \cos\alpha$$

The vertical displacement of the rail foot centre, vertical displacement of the sleepers and horizontal displacement of the rail head and foot along the longitudinal track axis are shown in Figs 21 - 30 [p. 32 - 41]. All graphs deal with loading case No. 6 and with the central sleeper in the modelled track section only.

The stress in the pad and rail foot deformation is shown in Figs 31 - 34 [p. 42 - 45] for the most dangerous loading case, No. 6. Results are given for both linear and non-linear assumptions of fastening system behaviour.

Tabs. 2 - 7 [p. 47 - 52] give the linear and non-linear computation results for loading cases 2, 4, 5 and 6. The definition and terminology of the relative deformative quantities are given in Technical Document ERRI D 170/DT 276. There is only one difference in the head rotation definition: HC = (HP - HC)/146.5 mm · 180/π. The values apply to the central sleeper in the modelled track section only. Tabs 6 and 7 [p. 51 and 52] show the difference between linear and non-linear model results, for which the following expression applies:

$$\% = \frac{nonlin - lin}{lin} \cdot 100\% \qquad \textbf{(32)}$$

The distribution coefficient for sleeper loading (g, computed using the following formula:

$$g = \frac{X_z}{Q} \qquad \textbf{(33)}$$

is greater for non-linear computation. This is shown in Tab. 8 [53].

3 BIBLIOGRAPHY

Vladimír Křístek, "Theory of box girders", Willey 1979, USA, 371 p.

ERRI D 170/DT 283	BASIC CONCEPT OF THE "SMALL MODEL"	Fig. 1

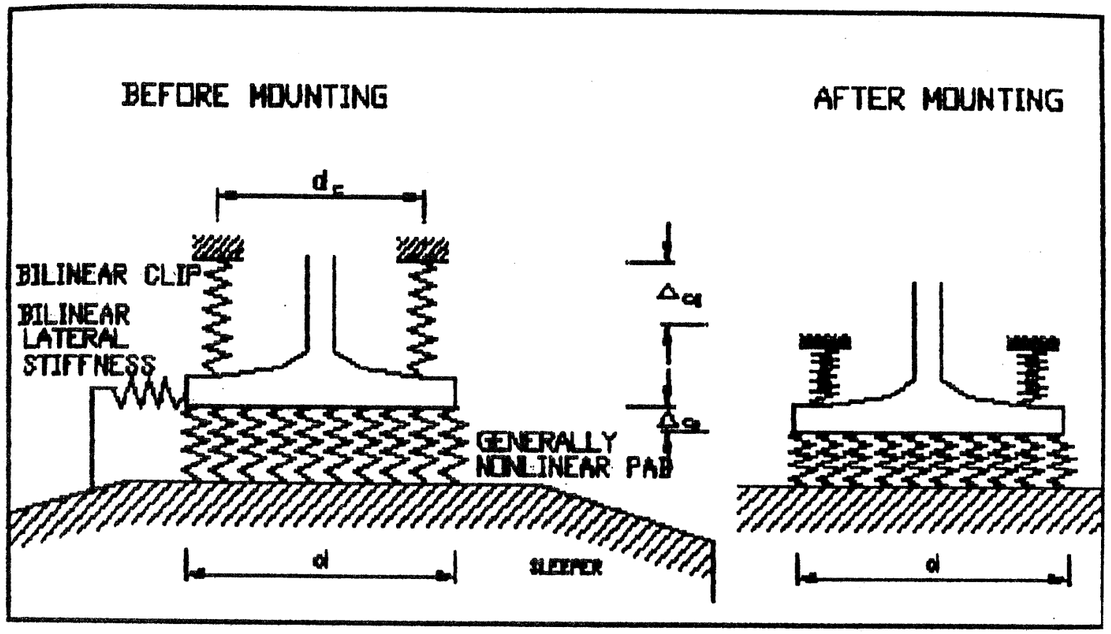

ERRI D 170/DT 283	IDEALIZED PRESENTATION OF ELASTIC PROPERTIES OF A RAIL PAD	Fig. 2

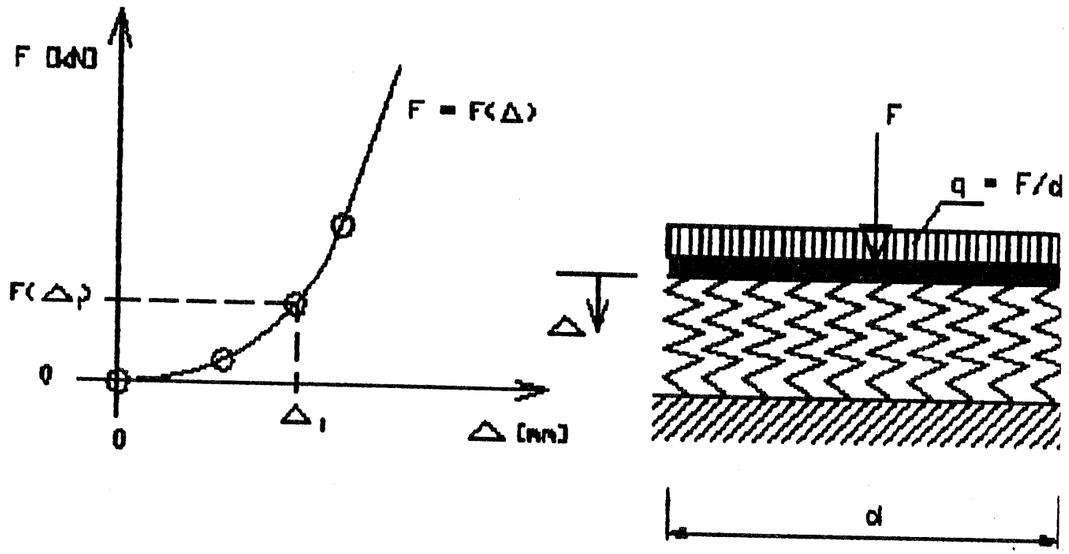

ERRI D 170/DT 283	INPUT DATA FOR THE NON-LINEAR MODEL STIFFNESS OF PADS (PART 1)	Fig. 3

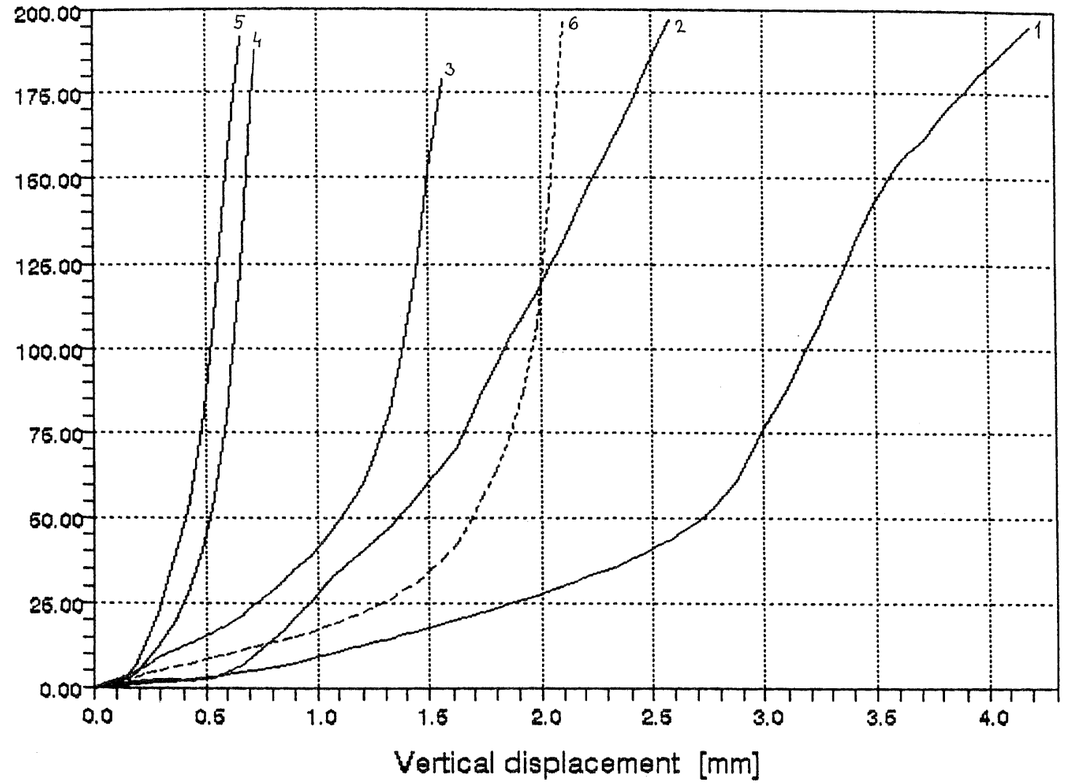

1 BR Pandrol

2 ZW 700

3 SNCF 9

4 SNCF 4.5

5 ZW687a

6 Pandrol quick

ERRI D 170/DT 283	INPUT DATA FOR THE NON-LINEAR MODEL STIFFNESS OF PADS (PART 2)	Fig. 4

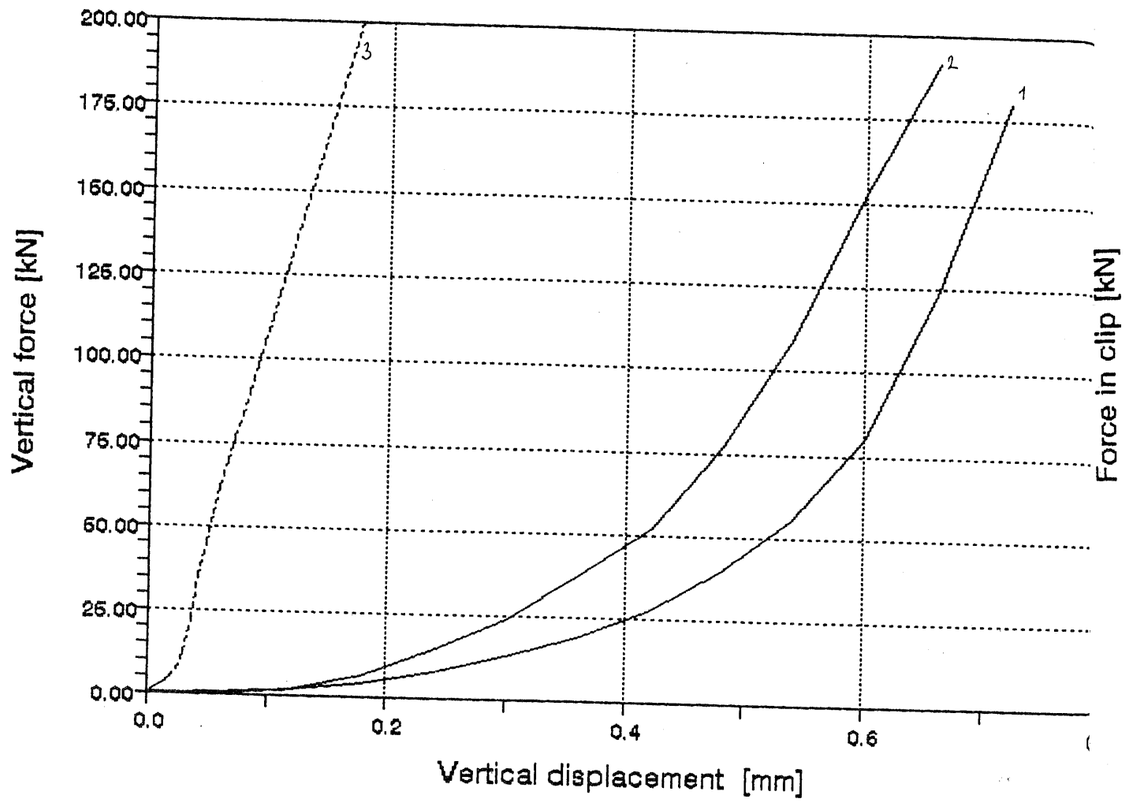

1 SNCF 4.5

2 ZW687a

3 ZW687a quick

ERRI D 170/DT 283	INPUT DATA FOR THE NON-LINEAR MODEL STIFFNESS OF CLIPS	Fig. 5

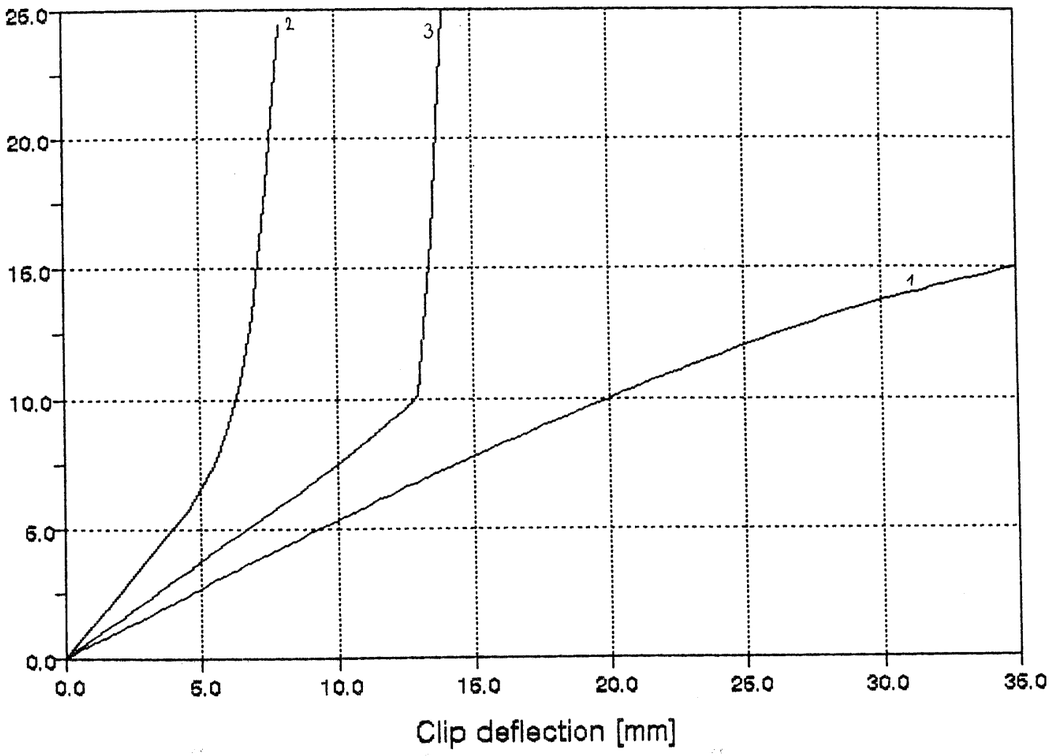

1 Pandrol

2 Nabla

3 Skl 14

ERRI D 170/DT 283	STRESS-STRAIN DIAGRAM FOR A SPRING REPRESENTING THE WHOLE FASTENING SYSTEM	Fig. 6

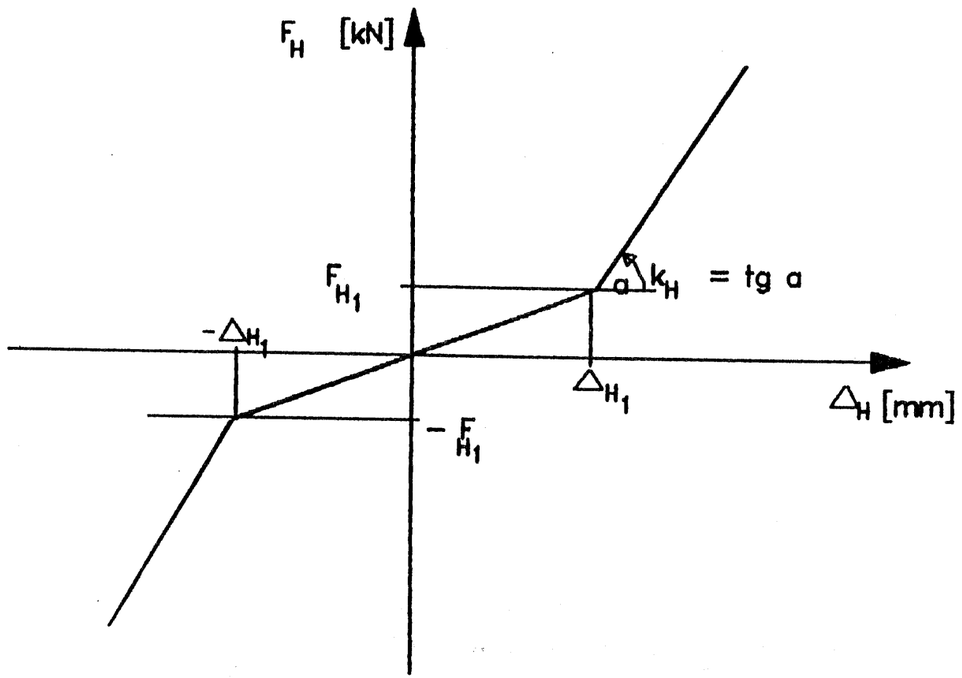

ERRI D 170/DT 283	RELATIONS BETWEEN FORCES AND DEFORMATIONS IN A FASTENING SYSTEM	Fig. 7

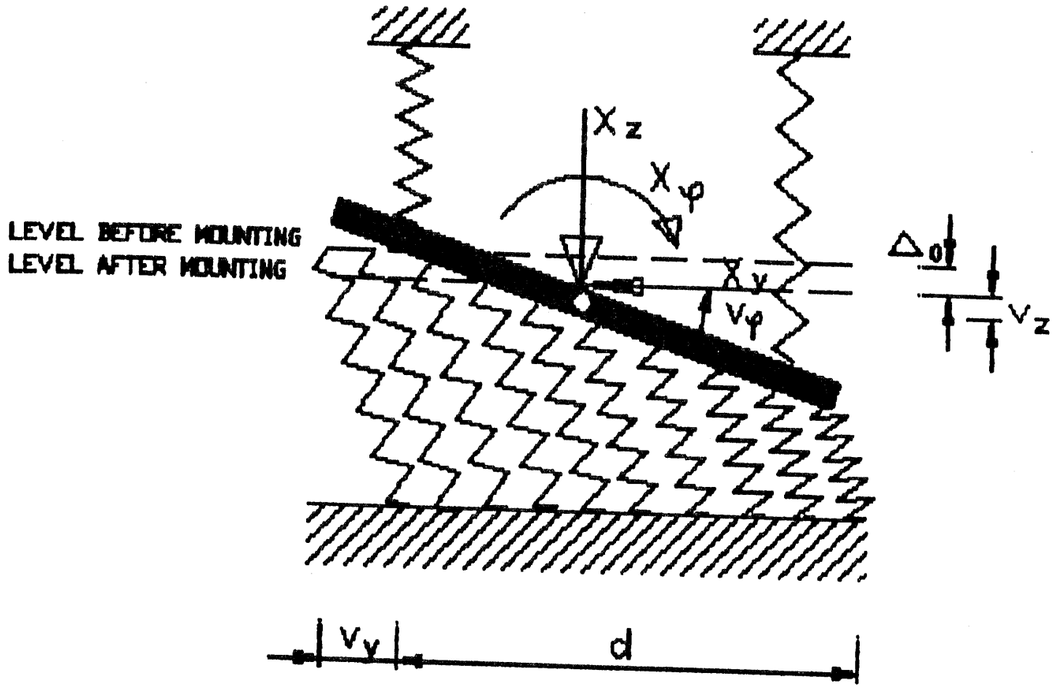

ERRI D 170/DT 283	GEOMETRIC RELATIONS EXPLAINING DEFORMATIONS OF A RAIL FOOT	Fig. 8

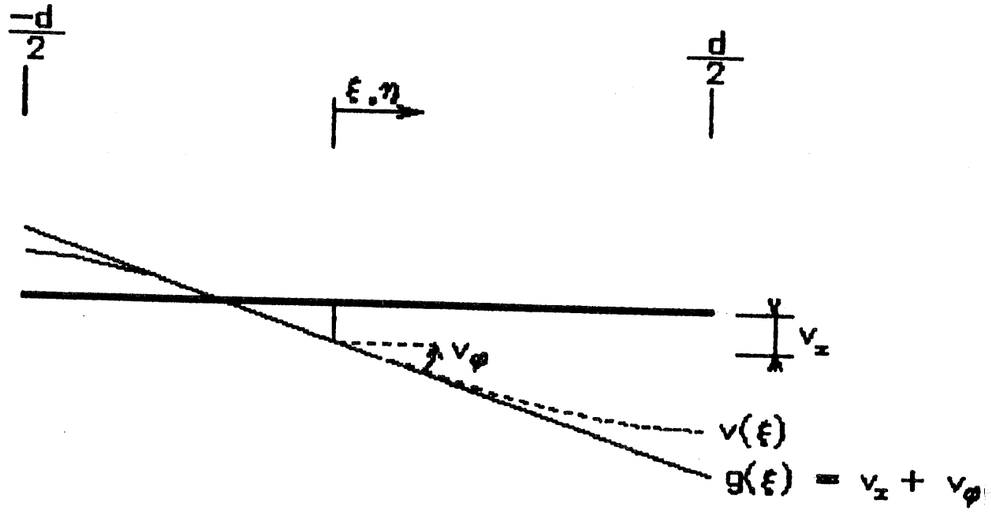

ERRI D 170/DT 283	FOLDED PLATE CROSS-SECTION REPRESENTING THE CROSS-SECTION OF THE UIC 60 RAIL	Fig. 9

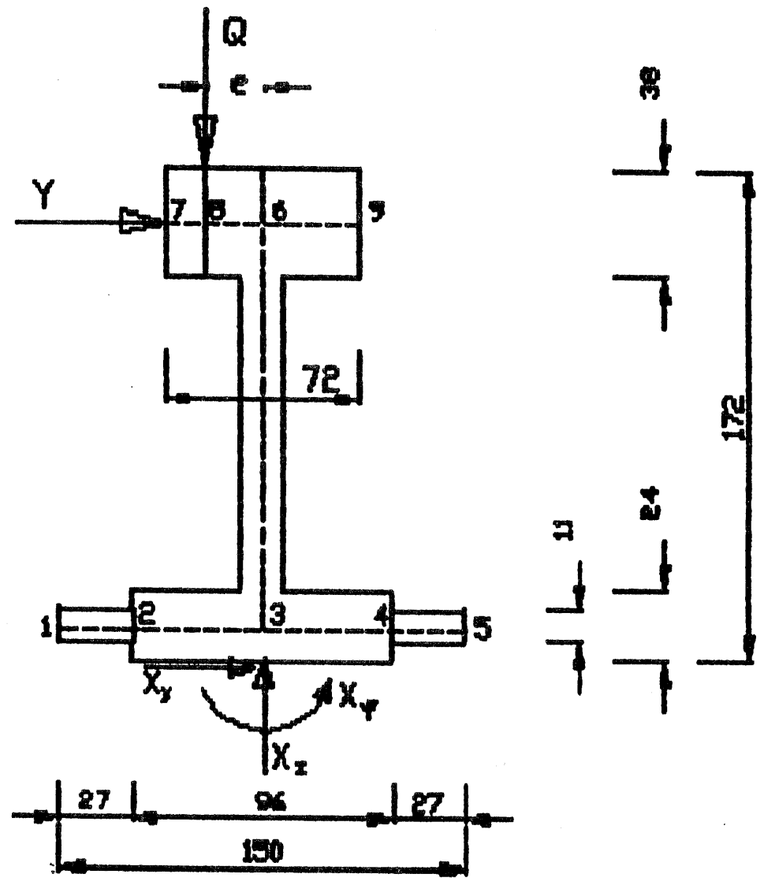

ERRI D 170/DT 283	LOCAL DEFORMATIONS OF A RAIL FOOT	Fig. 10

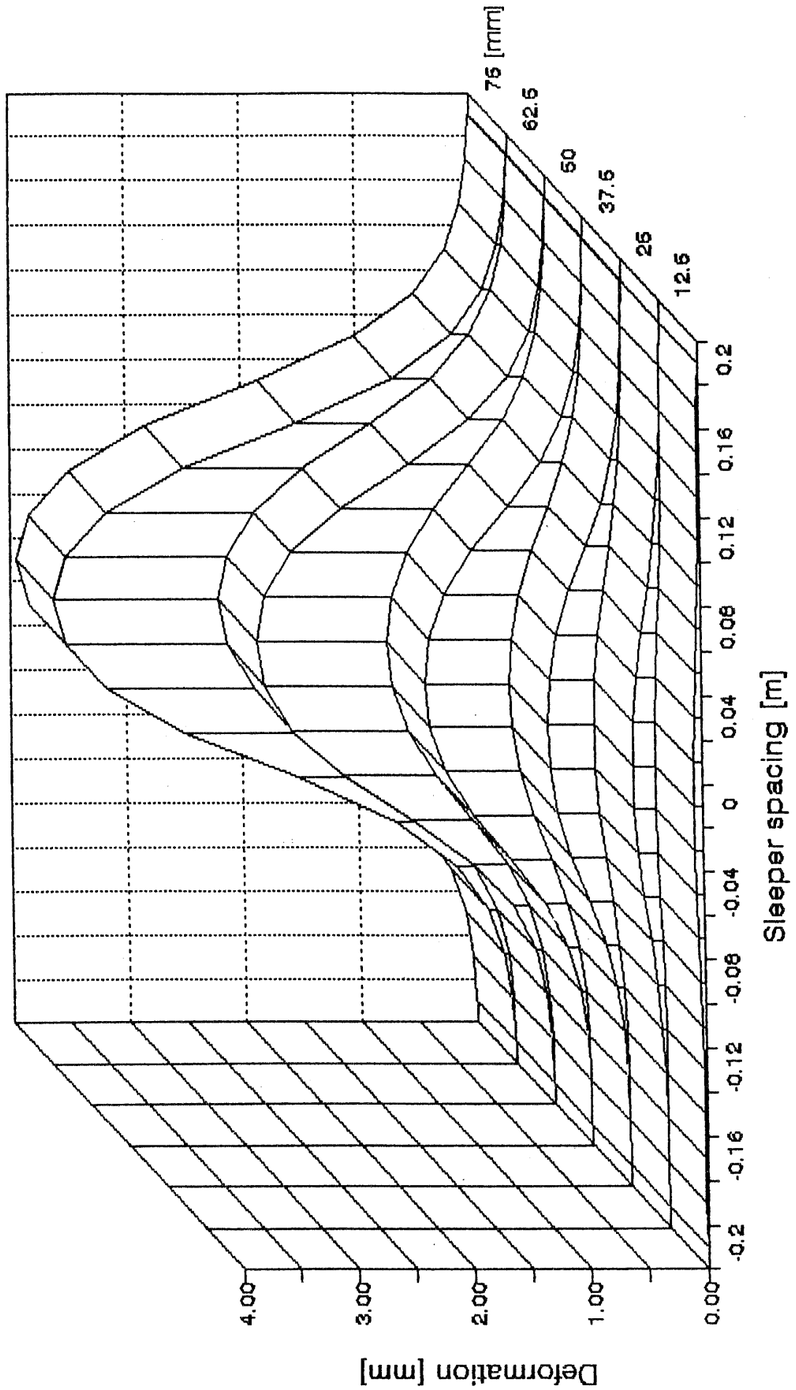

ERRI D 170/DT 283	CONTACT ZONE FOR DIFFERENT FASTENING SYSTEMS WITH SOFT RAIL PADS	Fig. 11

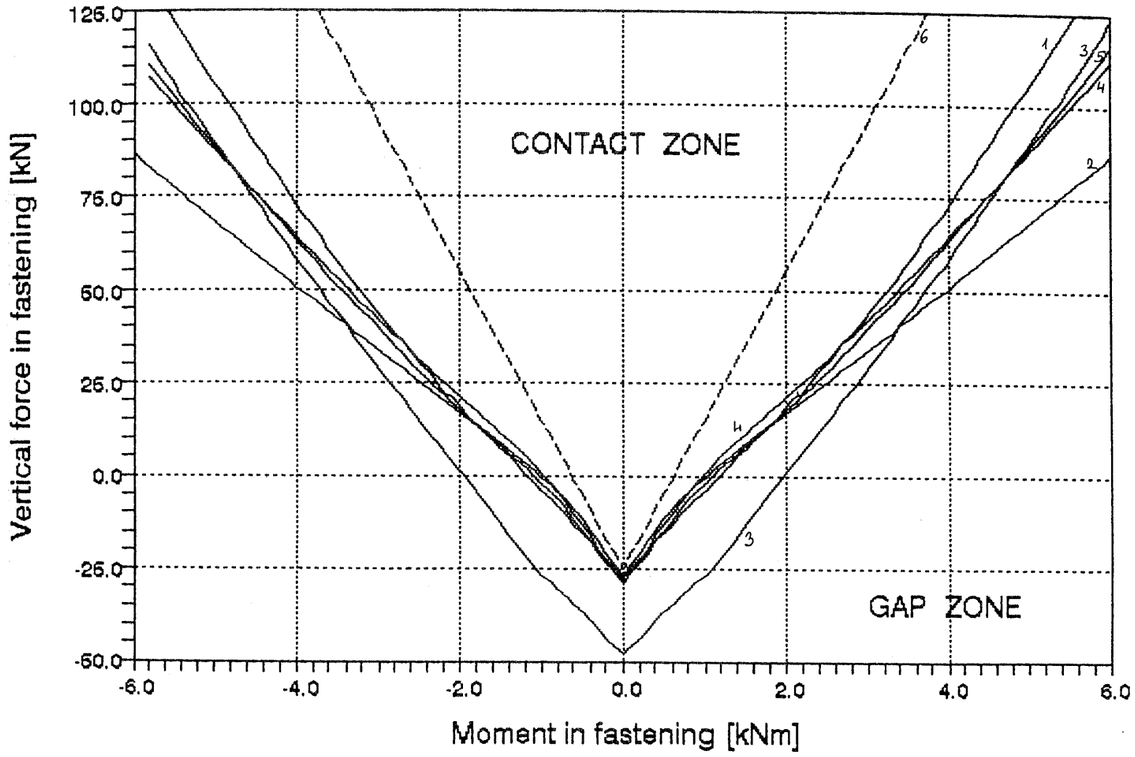

1 Pandrol

2 Pandrol. q

3 ZW700

4 SNCF 9mm

5 SNCF 4.5mm

6 Lin. case

ERRI D 170/DT 283	CONTACT ZONE FOR DIFFERENT FASTENING SYSTEMS WITH HARD RAIL PADS	Fig. 12

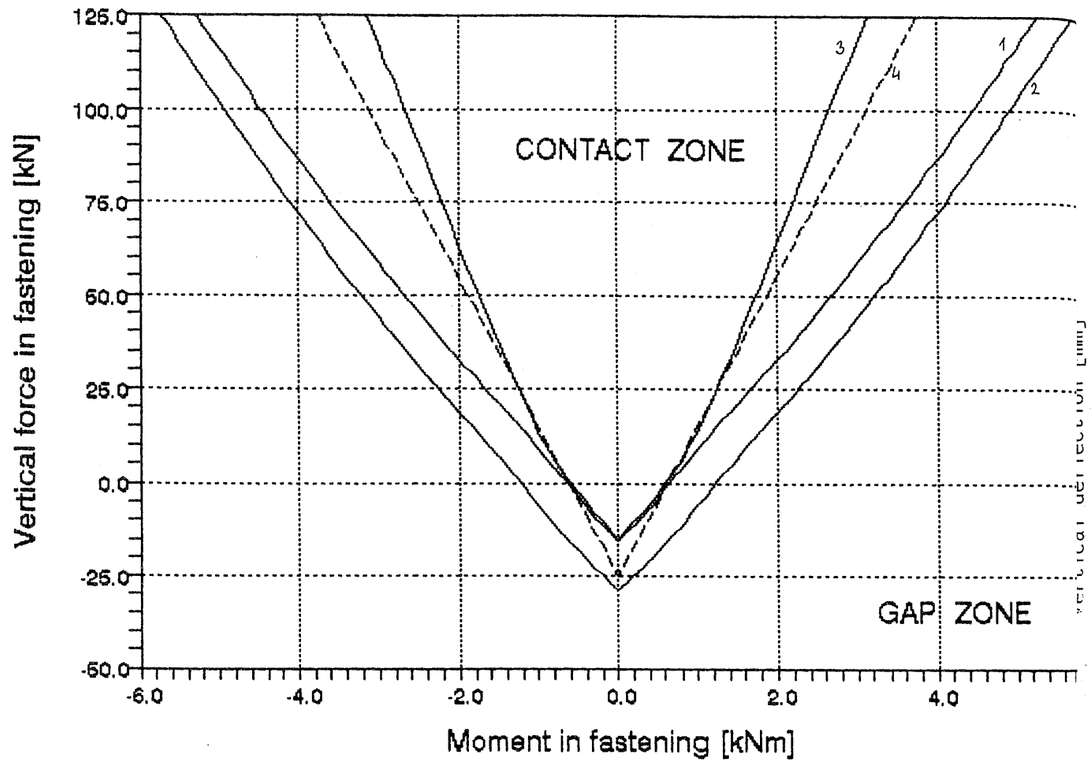

ERRI D 170/DT 283	RESULTS OF COMPUTER SIMULATION OF THE INCLINED TEST (PANDROL PAD; INCLINATION 30°)	Fig. 13

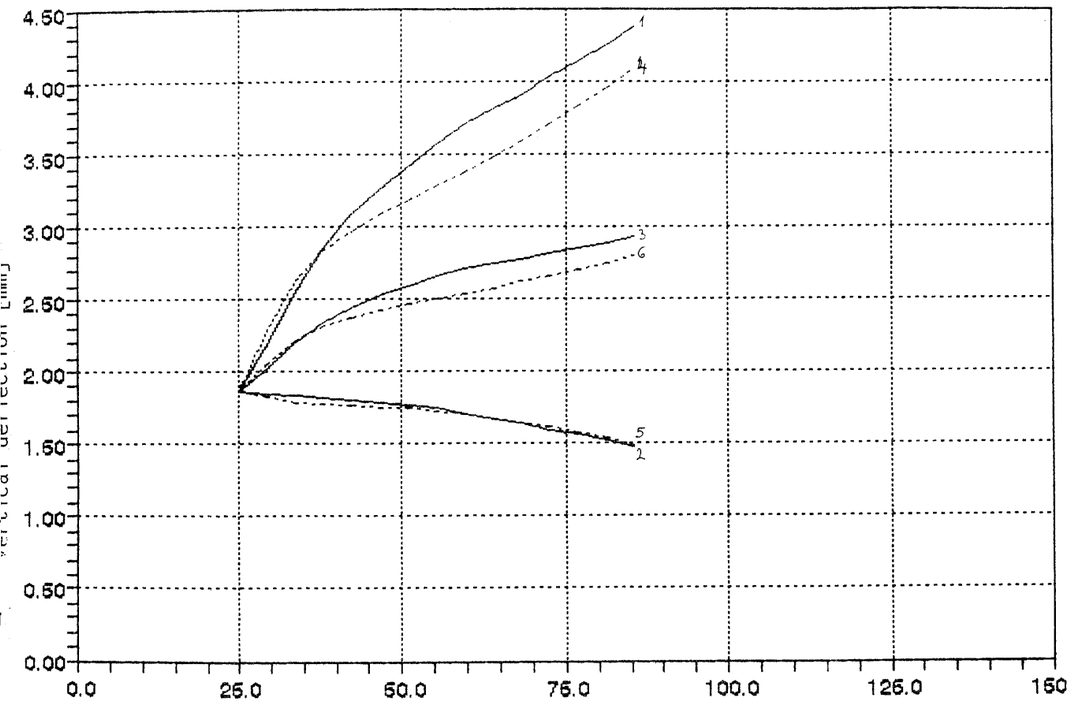

ERRI D 170/DT 283	RESULTS OF COMPUTER SIMULATION OF THE INCLINED TEST (ZW 700 PAD; INCLINATION 30°)	Fig. 14

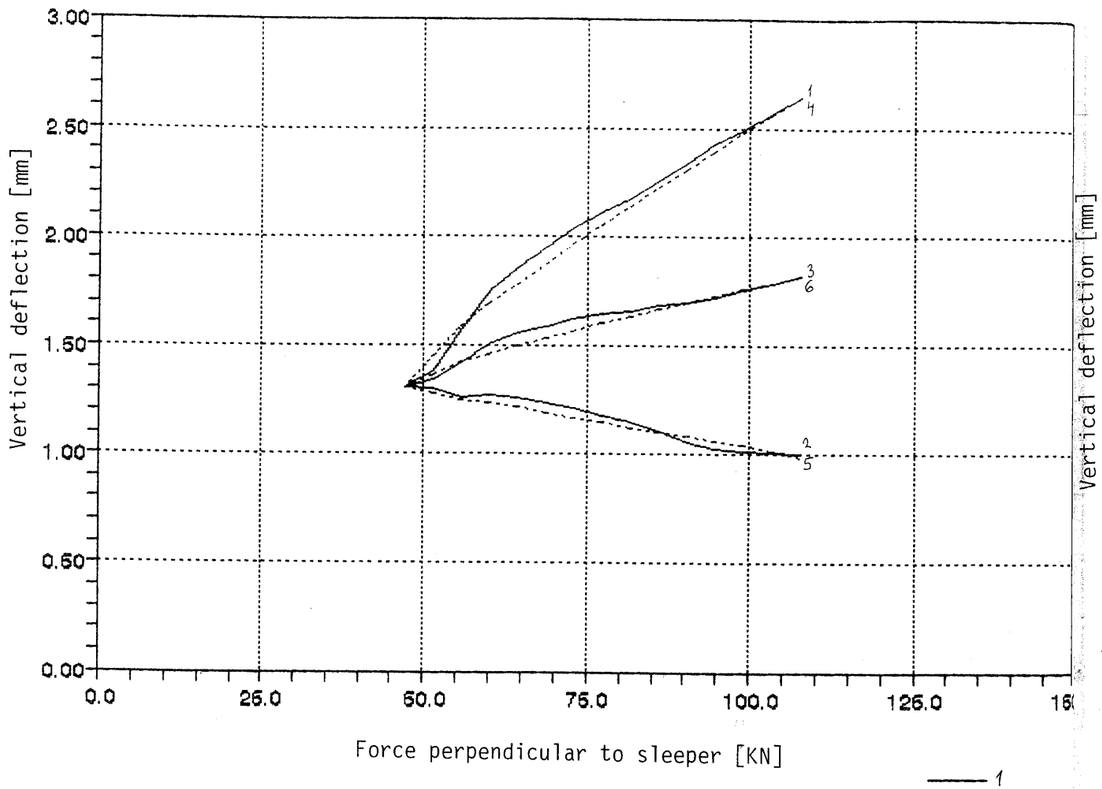

——— 1
VE ext.
——— 2
VI int.
——— 3
VC centre
-------- 4
VE calc.
-------- 5
VI calc.
-------- 6
VC calc.

ERRI D 170/DT 283	RESULTS OF COMPUTER SIMULATION OF THE INCLINED TEST (ZW 700 PAD; INCLINATION 40°)	Fig. 15

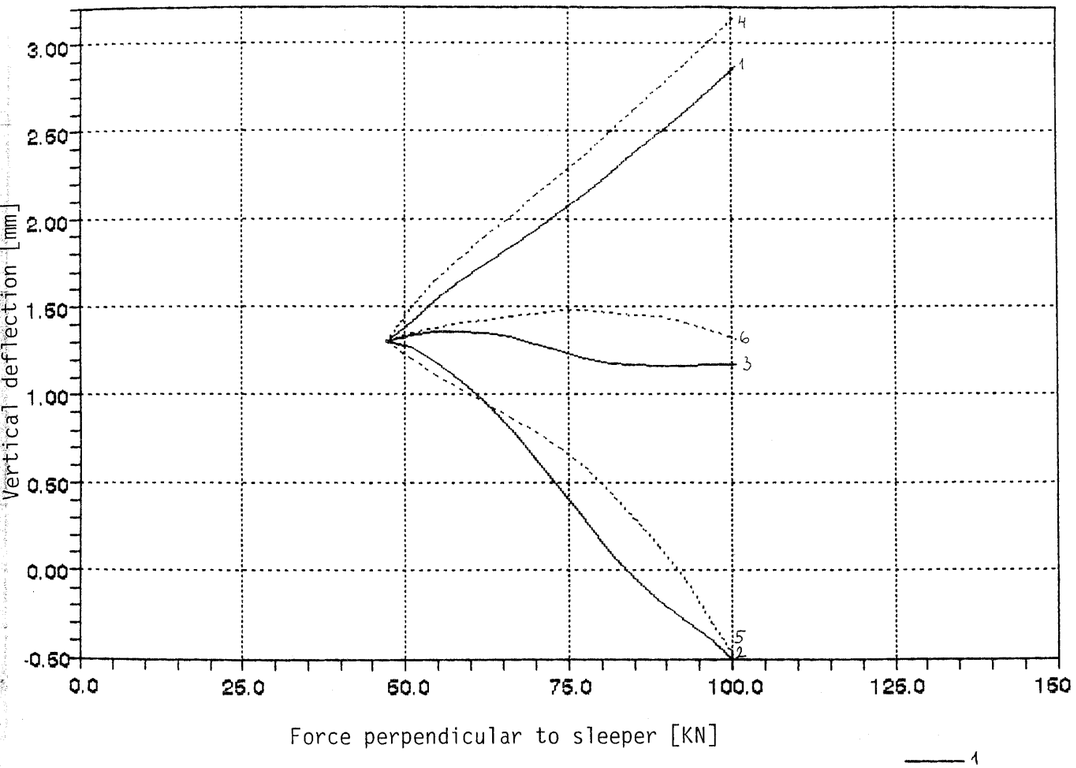

——— 1
VE ext.
——— 2
VI int.
——— 3
VC centre
-------- 4
VE calc.
-------- 5
VI calc.
-------- 6
VC calc.

ERRI D 170/DT 283	RESULTS OF COMPUTER SIMULATION OF THE INCLINED TEST (SNCF 9 mm PAD; INCLINATION 30°)	Fig. 16

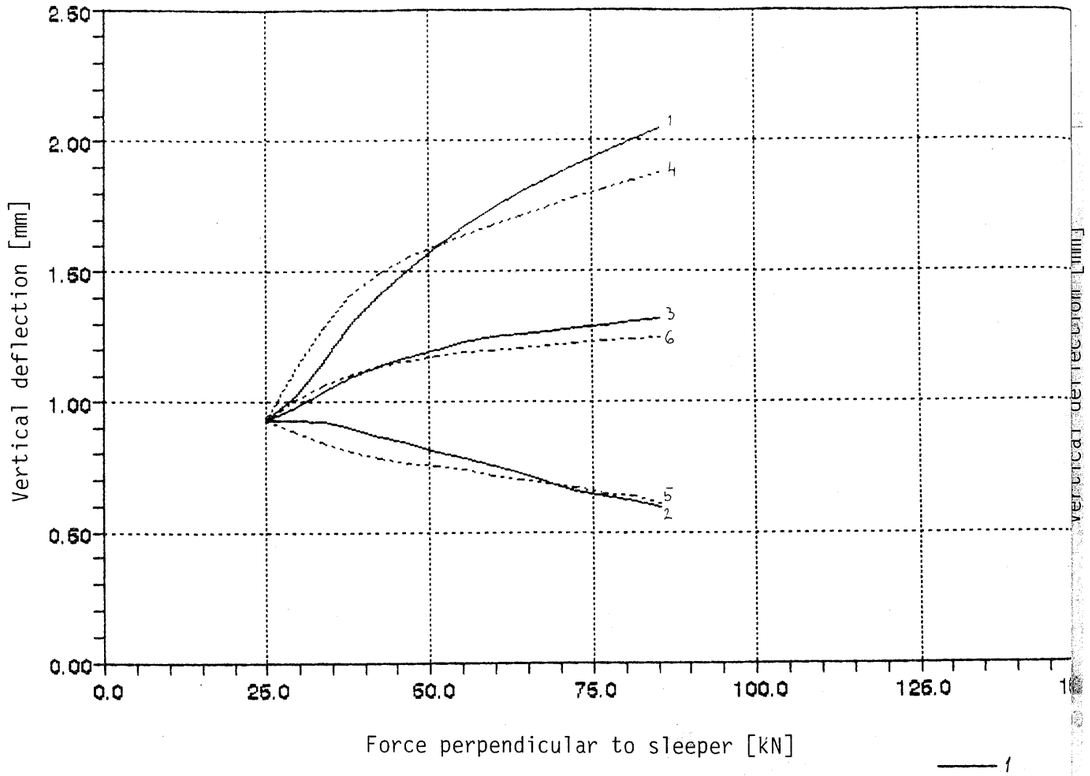

ERRI D 170/DT 283	RESULTS OF COMPUTER SIMULATION OF THE INCLINED TEST (SNCF 4.5 mm PAD; INCLINATION 30°)	Fig. 17

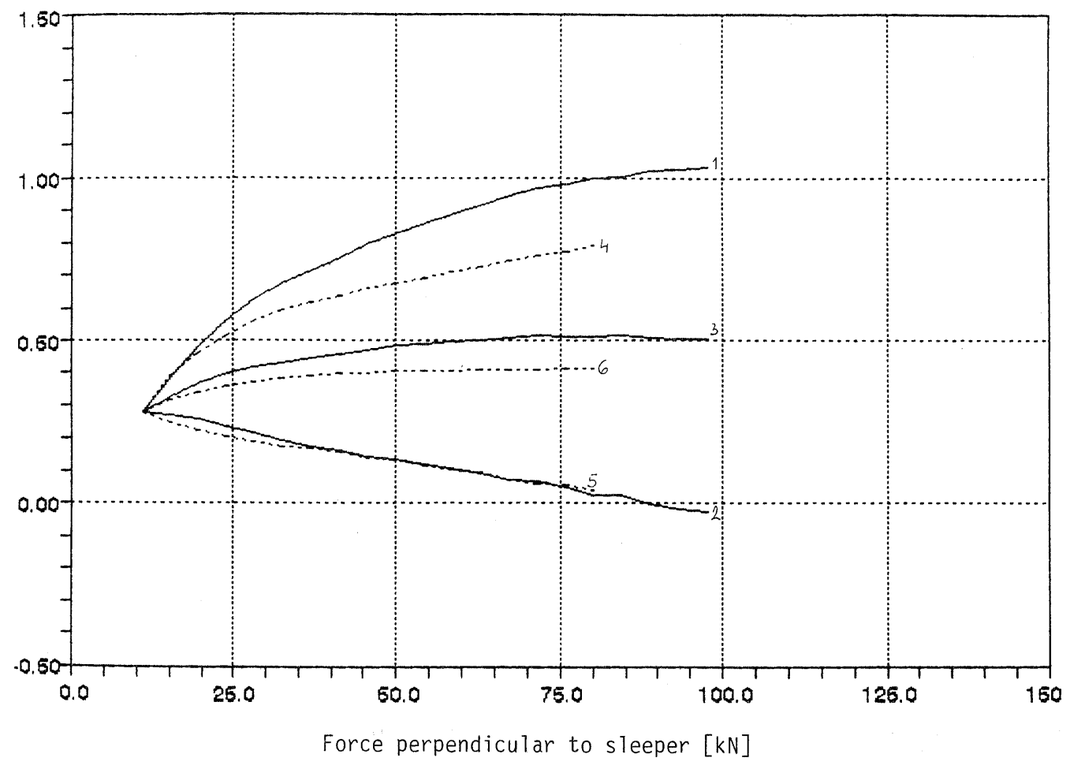

ERRI D 170/DT 283	RESULTS OF COMPUTER SIMULATION OF THE INCLINED TEST (SNCF 4.5 mm PAD; INCLINATION 40°)	Fig. 18

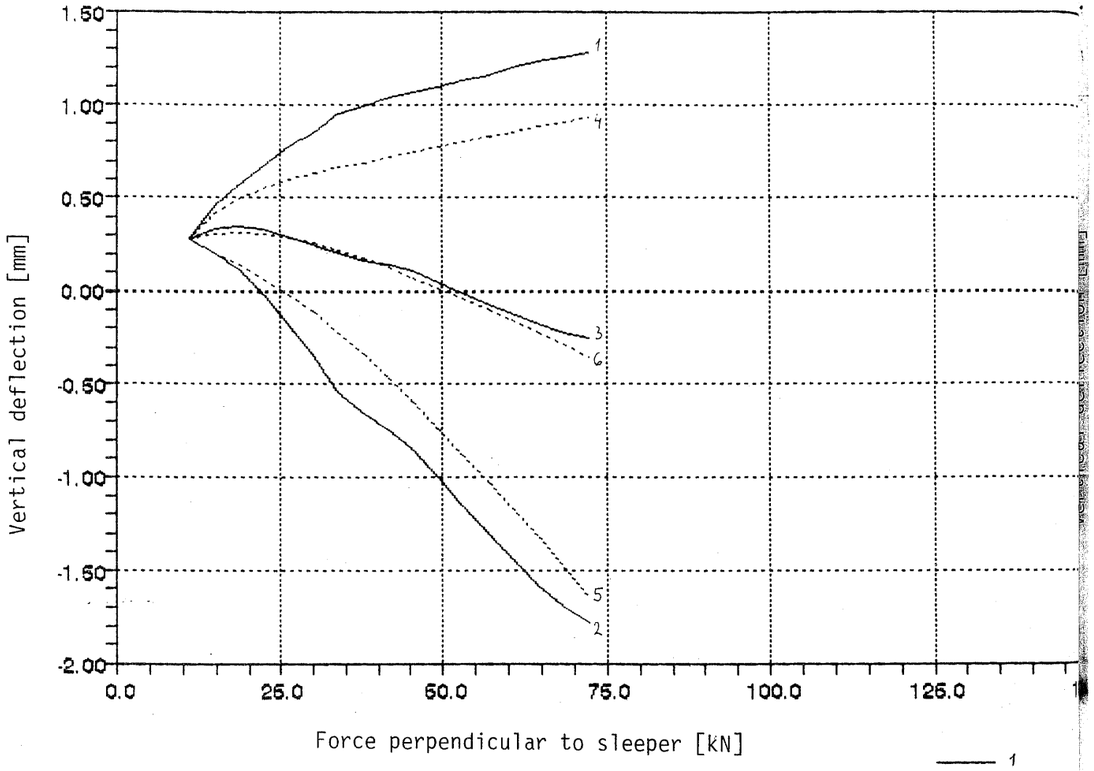

—— 1 VE ext.

—— 2 VI int.

—— 3 VC centre

-------4 VE calc.

-------5 VI calc.

-------6 VC calc.

ERRI D 170/DT 283	RESULTS OF COMPUTER SIMULATION OF THE INCLINED TEST (ZW 687a PAD; INCLINATION 30°)	Fig. 19

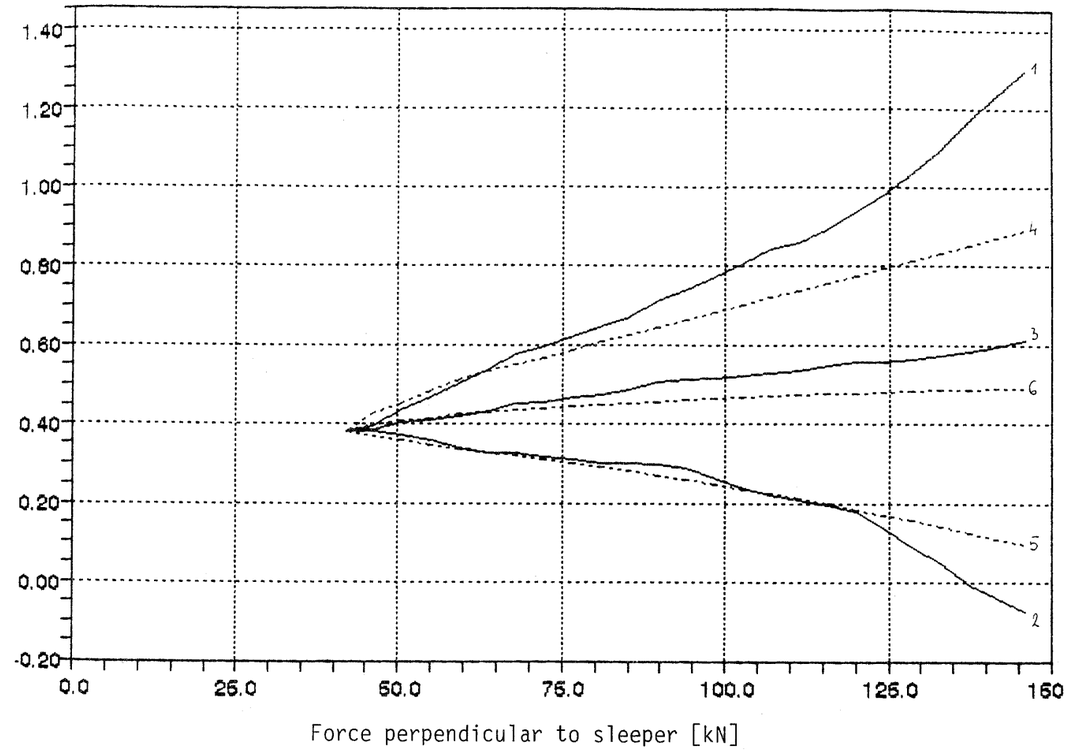

—— 1 VE ext.

—— 2 VI int.

—— 3 VC centre

-------4 VE calc.

-------5 VI calc.

-------6 VC calc.

ERRI D 170/DT 283	RESULTS OF COMPUTER SIMULATION OF THE INCLINED TEST (ZW 687a PAD; INCLINATION 40°)	Fig. 20

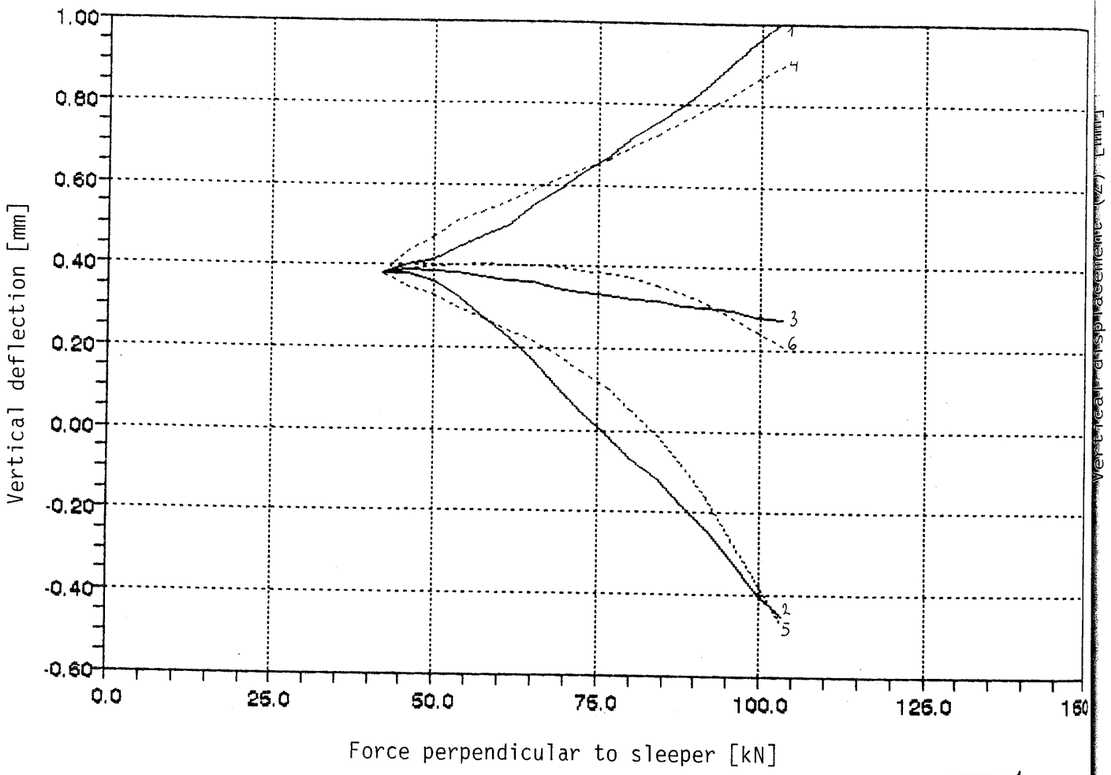

ERRI D 170/DT 283	COMPUTED VERTICAL TRACK DEFORMATIONS (PANDROL PAD)	Fig. 21

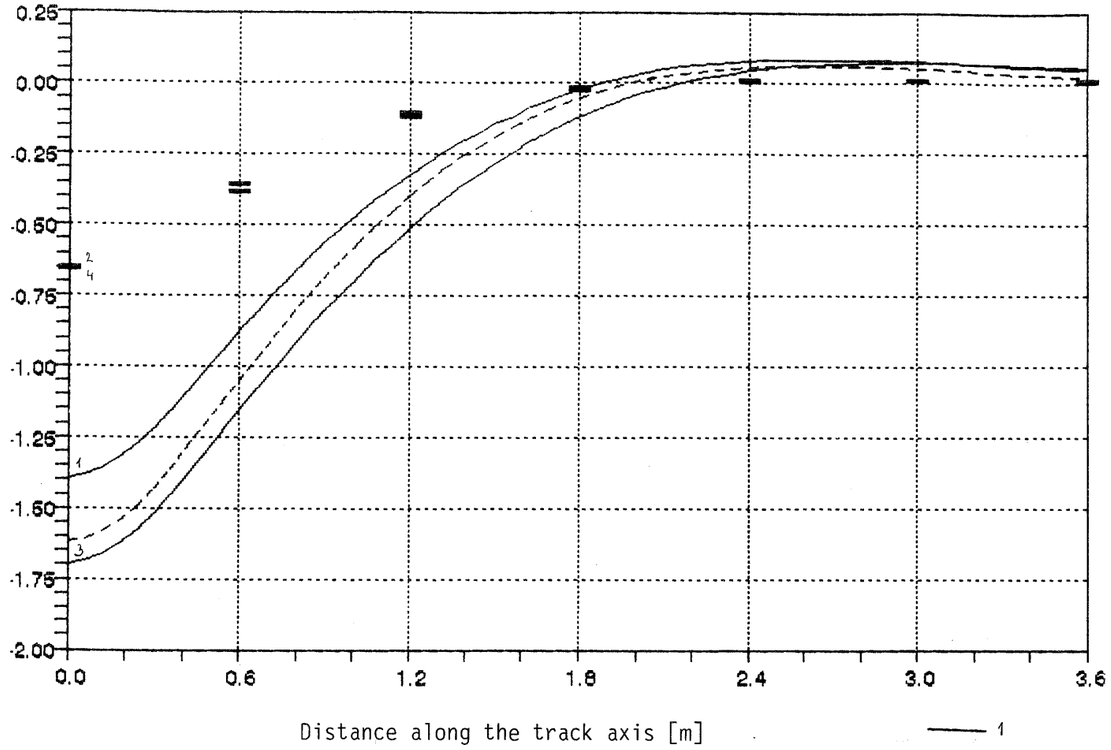

ERRI D 170/DT 283	COMPUTED LATERAL TRACK DEFORMATIONS (PANDROL PAD)	Fig. 22

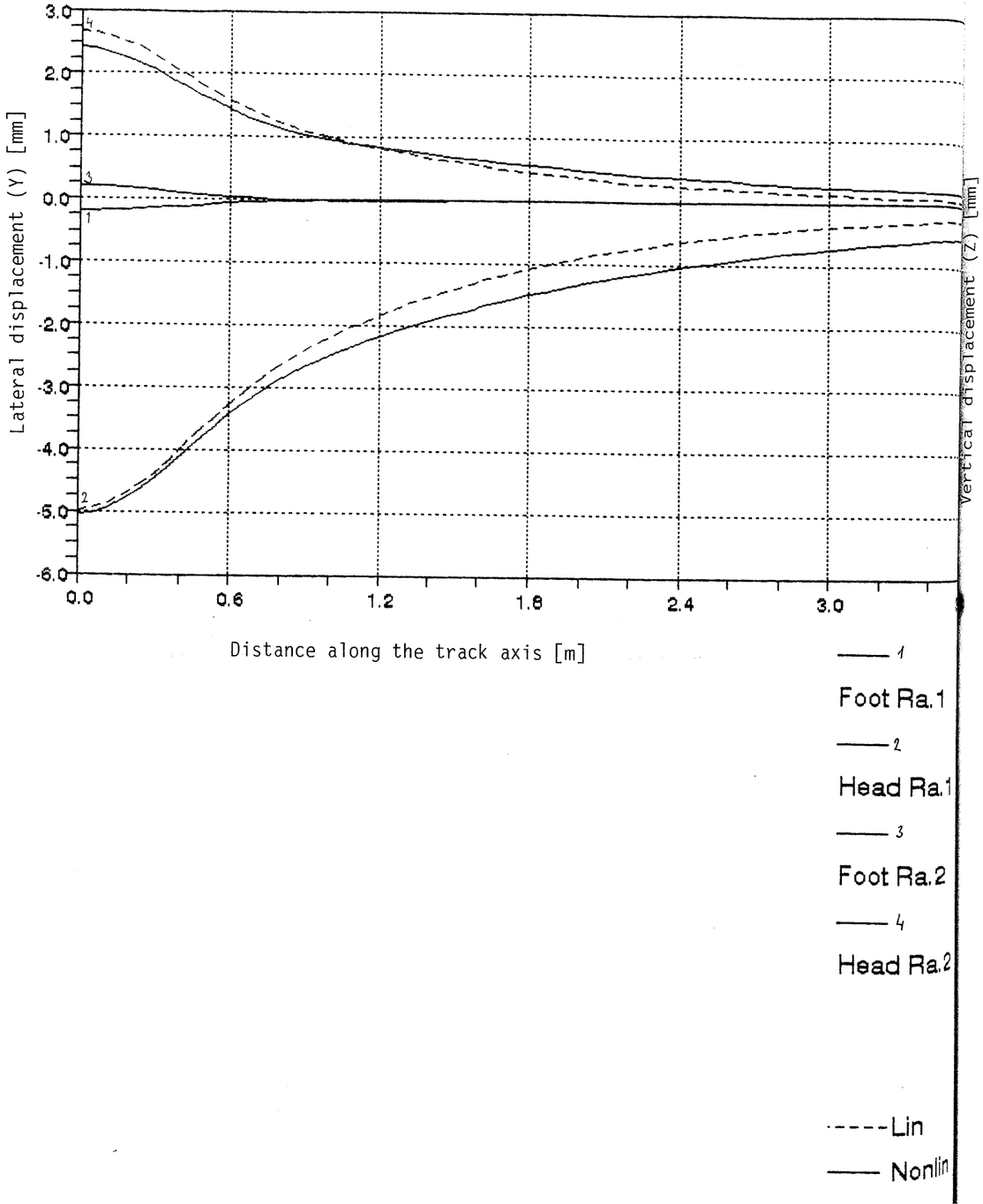

ERRI D 170/DT 283	COMPUTED VERTICAL TRACK DEFORMATIONS (ZW 700 PAD)	Fig. 23

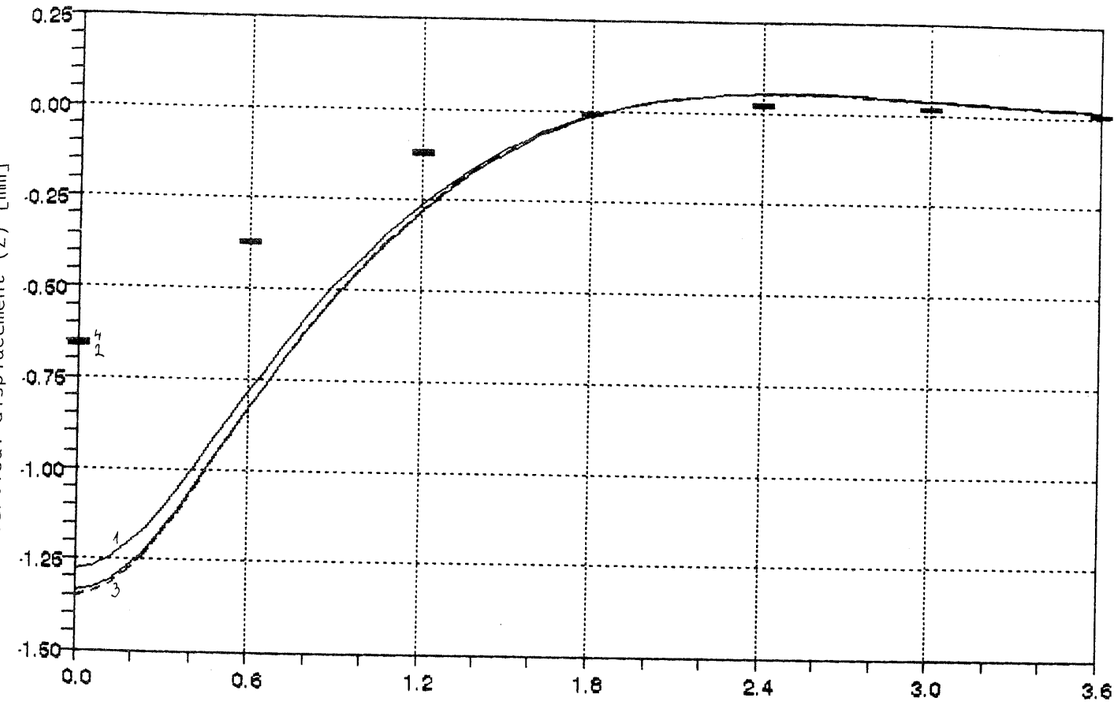

ERRI D 170/DT 283	COMPUTED LATERAL TRACK DEFORMATIONS (ZW 700 PAD)	Fig. 24

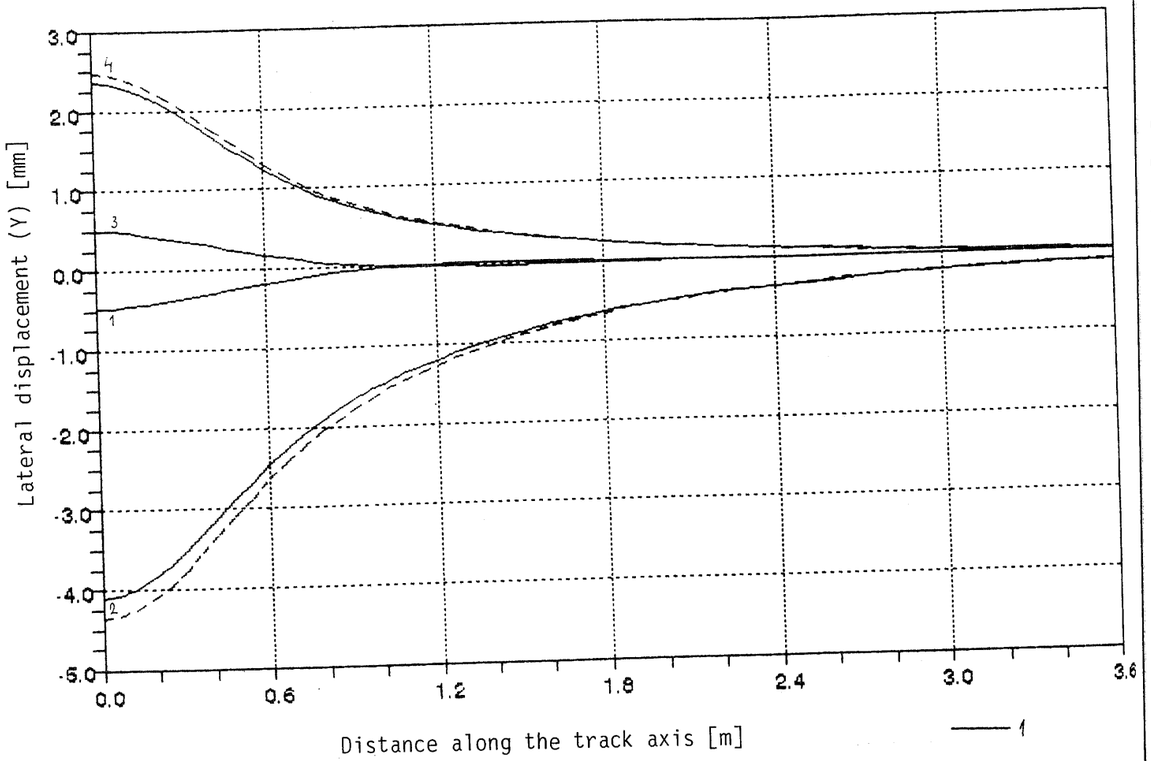

ERRI D 170/DT 283	COMPUTED VERTICAL TRACK DEFORMATIONS (SNCF 9 mm PAD)	Fig. 25

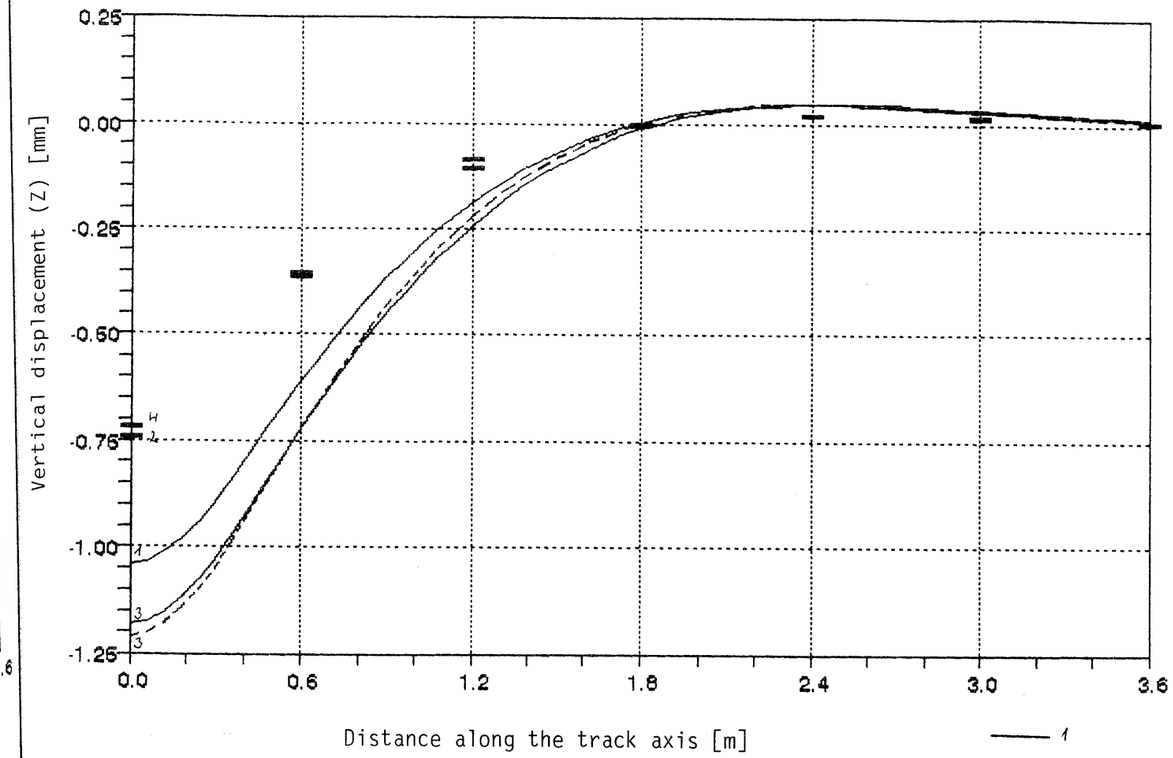

ERRI D 170/DT 283	COMPUTED LATERAL TRACK DEFORMATIONS (SNCF 9 mm PAD)	Fig. 26

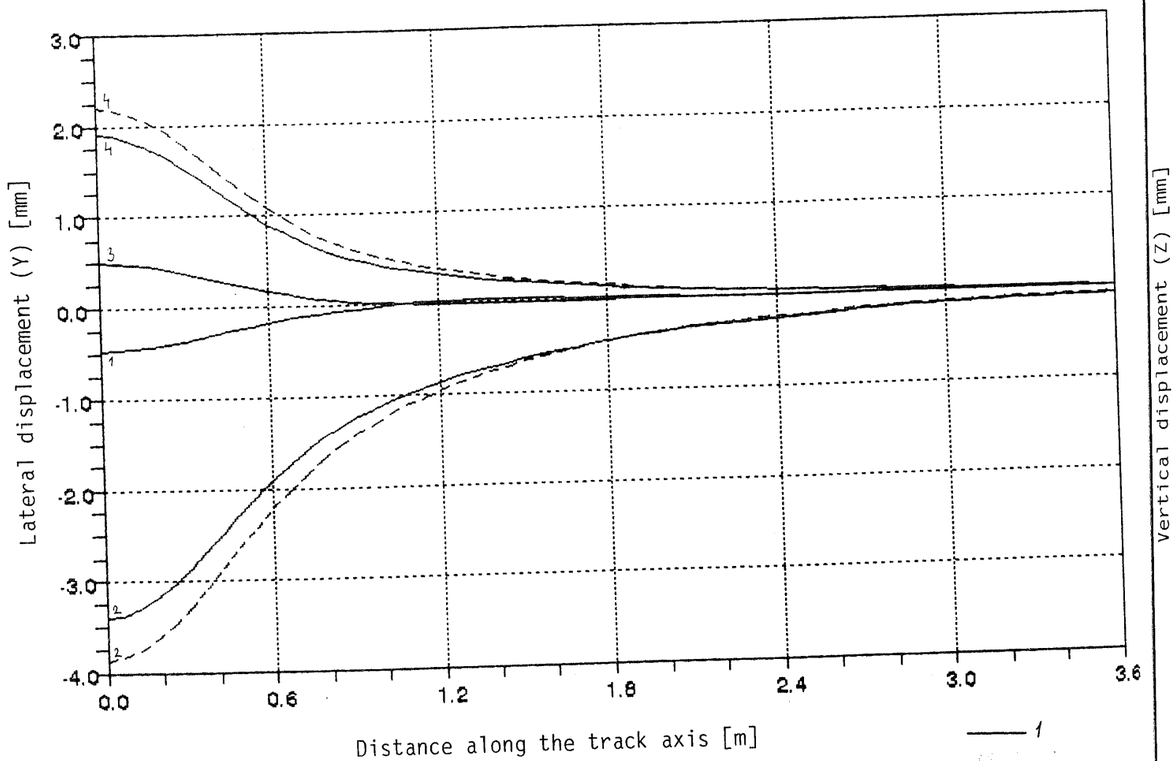

ERRI D 170/DT 283	COMPUTED VERTICAL TRACK DEFORMATIONS (SNCF 4.5 mm PAD)	Fig. 27

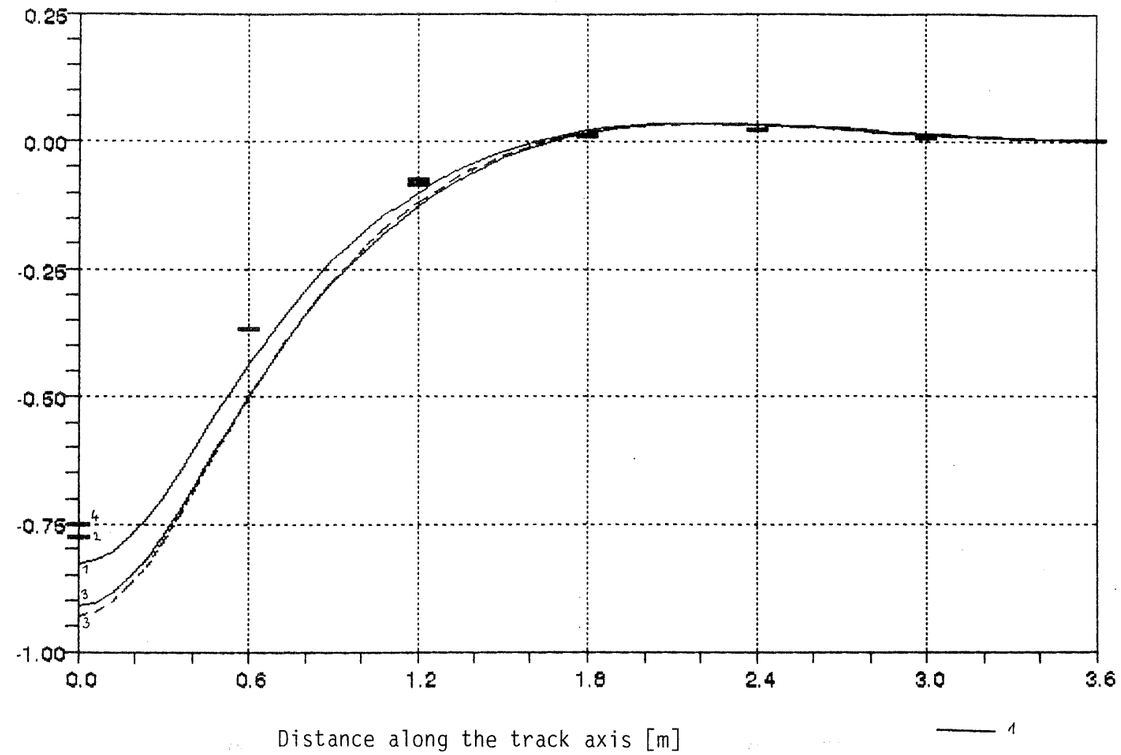

ERRI D 170/DT 283	COMPUTED LATERAL TRACK DEFORMATIONS (SNCF 4.5 mm PAD)	Fig. 28

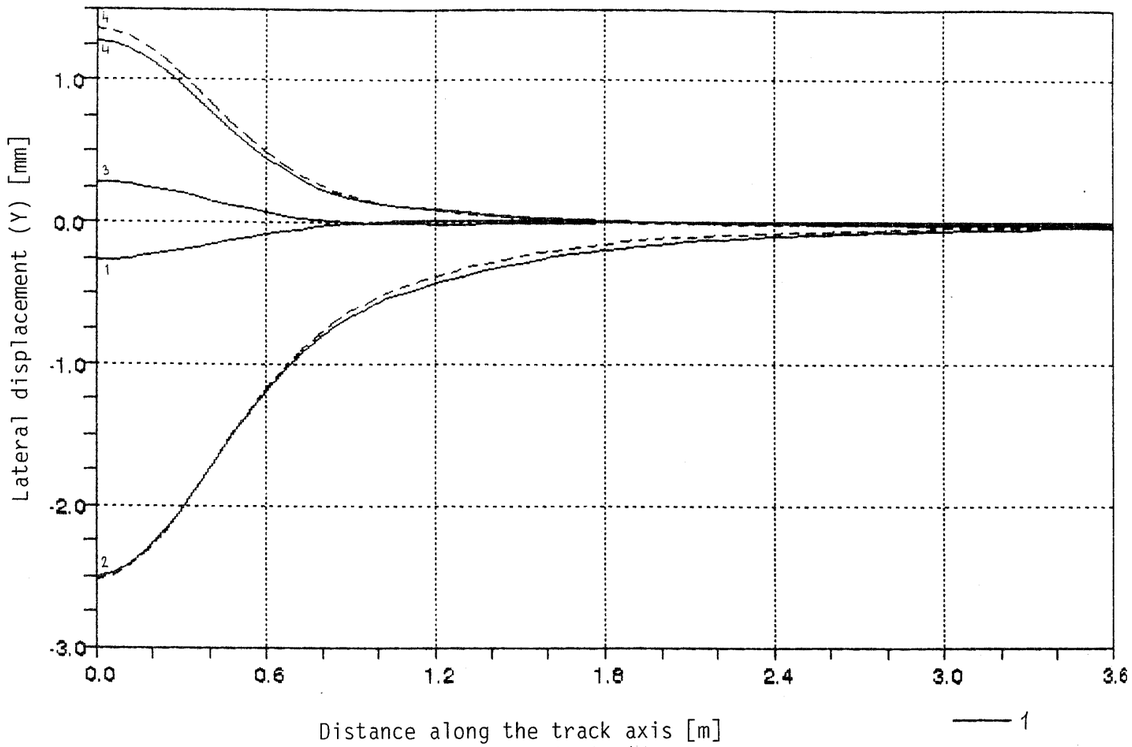

ERRI D 170/DT 283	COMPUTED VERTICAL TRACK DEFORMATIONS (ZW 687a PAD)	Fig. 29

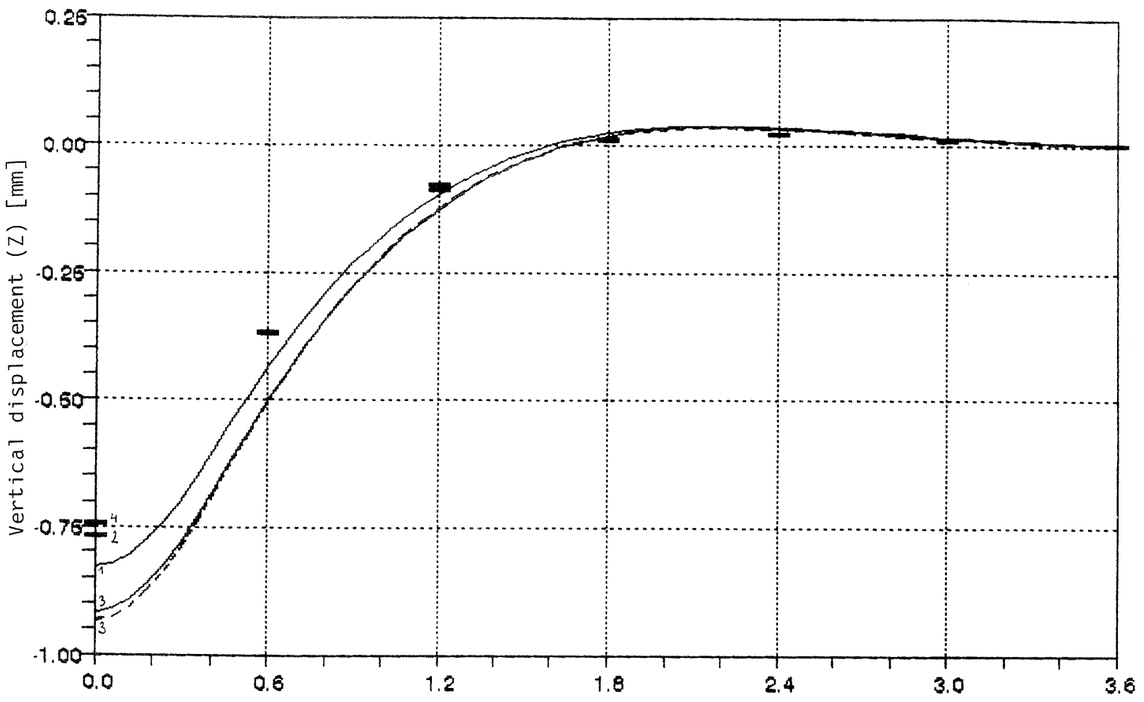

ERRI D 170/DT 283	COMPUTED LATERAL TRACK DEFORMATIONS (ZW 687a PAD)	Fig. 30

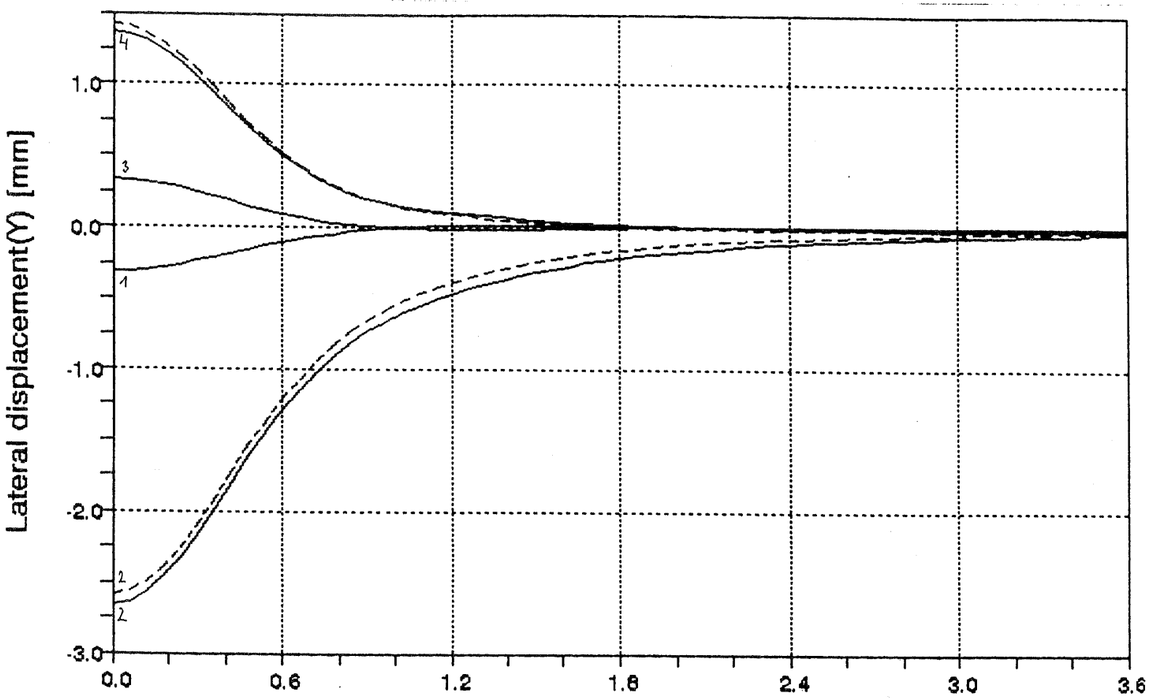

1 Foot Ra.1

2 Head Ra.1

3 Foot Ra.2

4 Head Ra.2

-----Lin

—— Nonlin

ERRI D 170/DT 283	RESULTS OF THE LINEAR COMPUTATION OF STRESSES IN PADS	Fig. 31

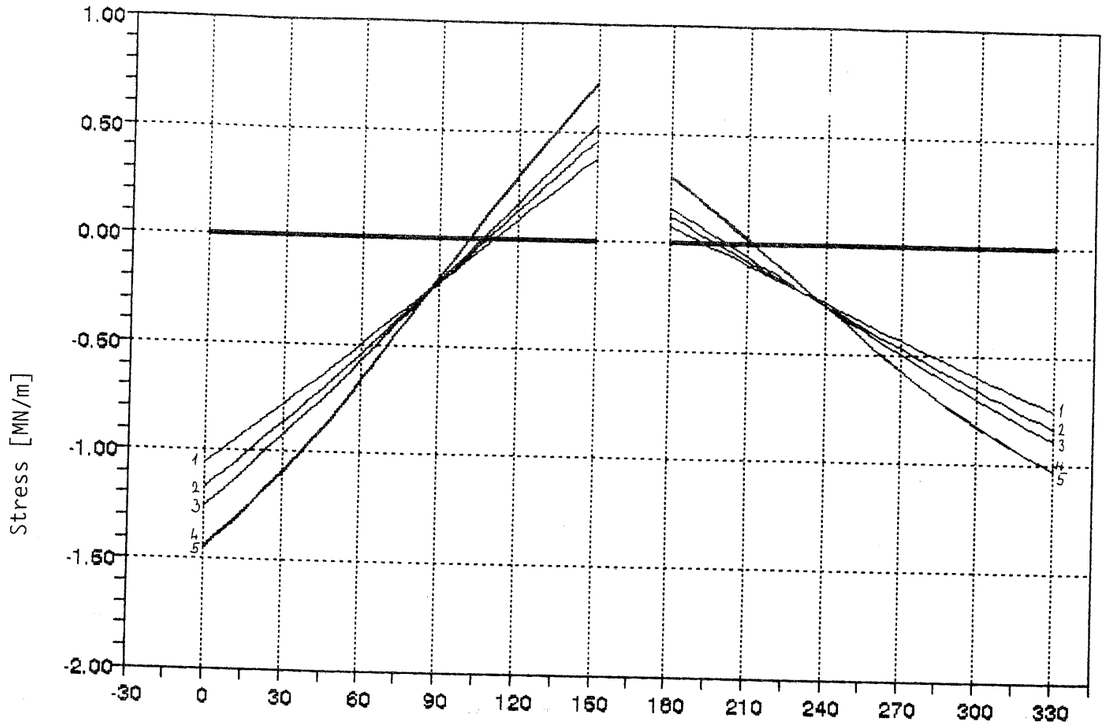

Distance along a pad in the direction perpendicular to the axis of the rail [mm]

1 BR Pandrol

2 ZW700

3 SNCF 9mm

4 SNCF 4.5mm

5 ZW687a 20kN

ERRI D 170/DT 283	RESULTS OF NON-LINEAR COMPUTATION OF STRESSES IN PADS	Fig. 32

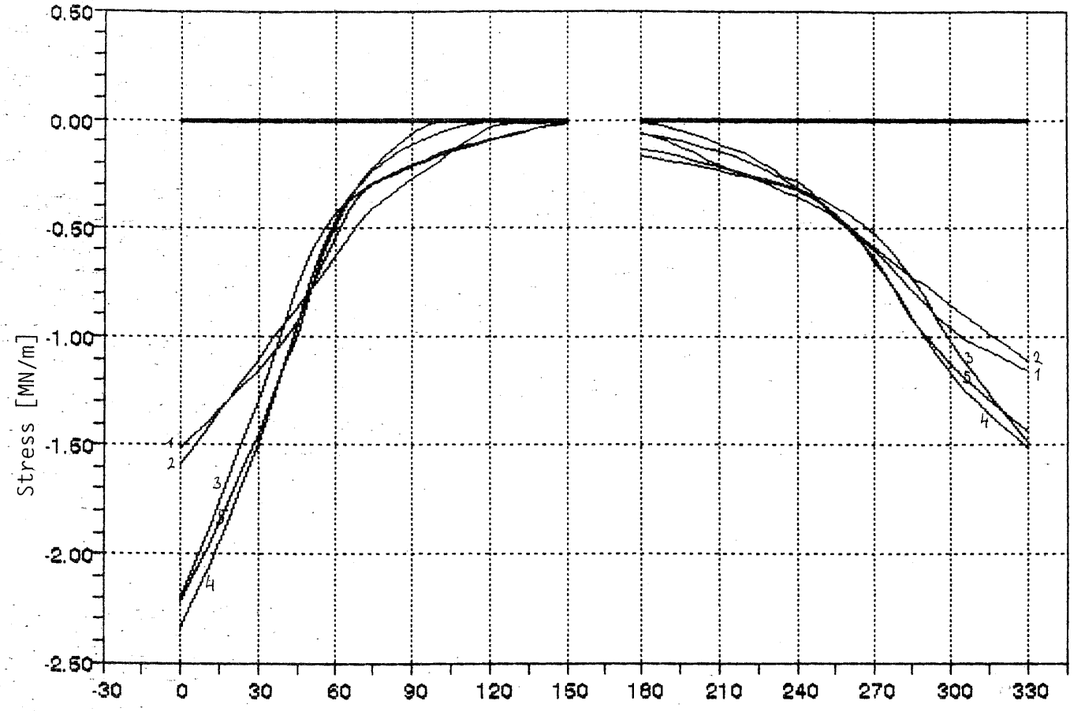

ERRI D 170/DT 283	RESULTS OF LINEAR COMPUTATIONS OF RAIL FOOT DEFORMATIONS	Fig. 33

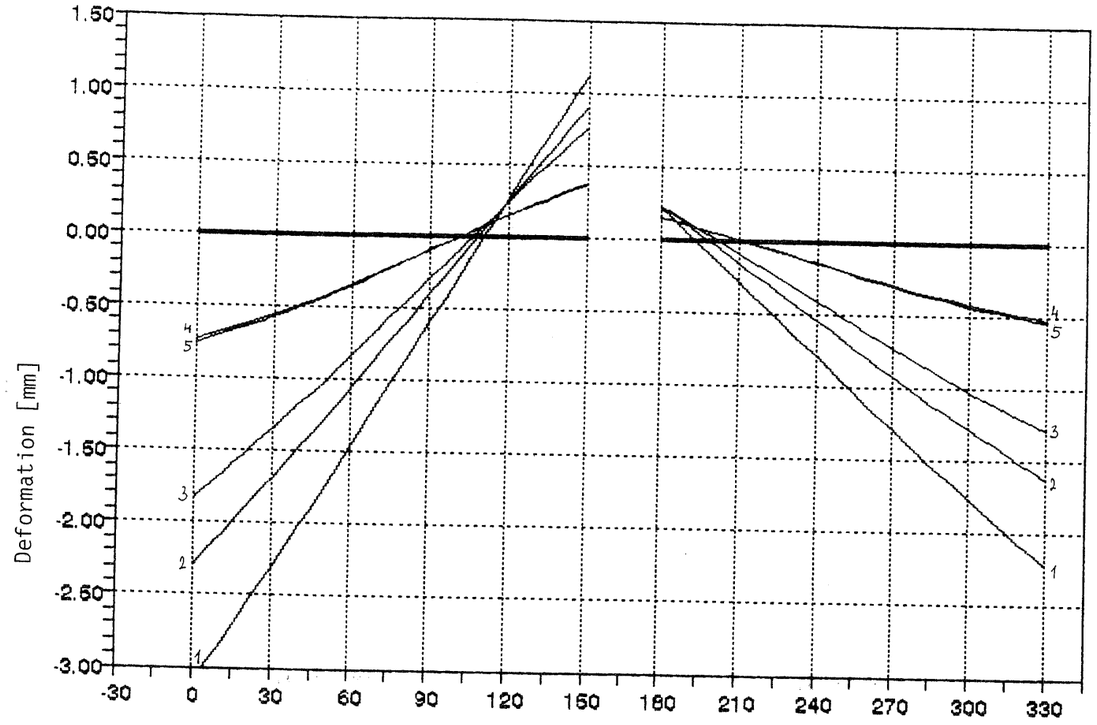

ERRI D 170/DT 283	RESULTS OF NON-LINEAR COMPUTATIONS OF RAIL FOOT DEFORMATIONS	Fig. 34

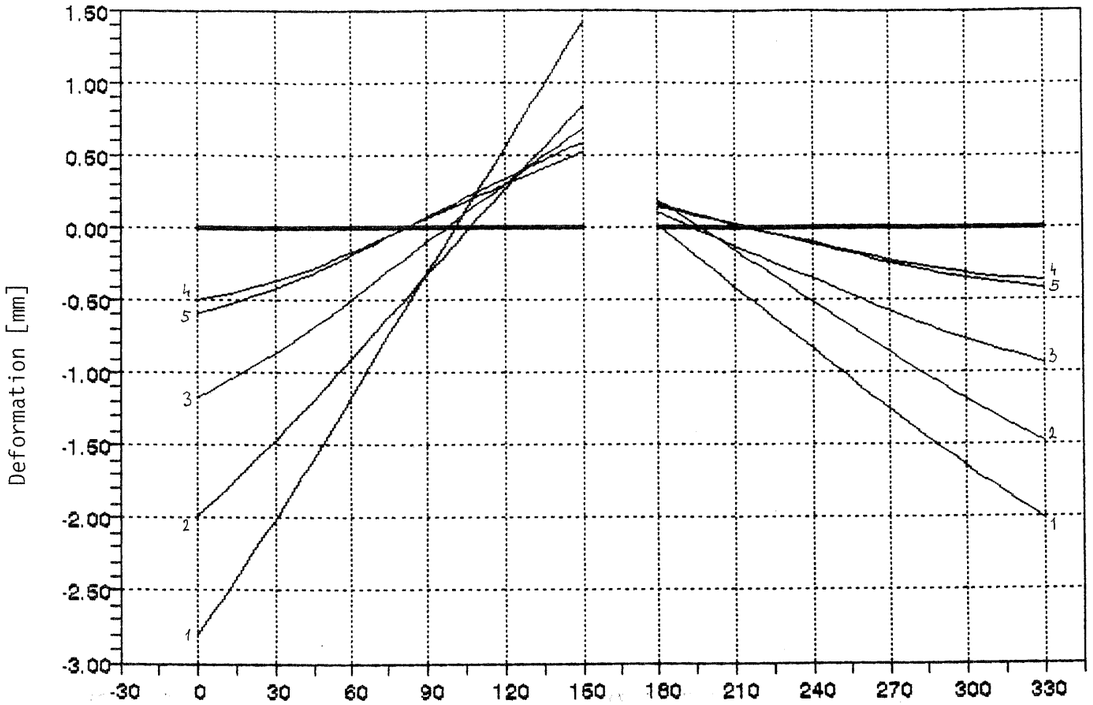

Distance along a pad in the direction perpendicular to the axis of the rail [mm]

—— 1
BR Pandrol

—— 2
ZW700

—— 3
SNCF 9mm

—— 4
SNCF 4.5mm

—— 5
ZW687a 20kN

ERRI D 170/DT 283	INPUT DATA FOR LINEAR AND NON-LINEAR COMPUTATIONS	Tab. 1

Pad and compression case	$k_{pad,\ lin}$ [MN/m]	k_{lin} [MN/m]	Clip	k_{lat} [kN/mm]	Toe load [kN]
Pandrol	50	51.1	Pandrol	250	25
Pandrol q	95	96.1	Pandrol	250	25
ZW 700	75.2	76.7	Skl 14	90	20
SNCF 9 mm	100	103.1	Nabla	90	25
SNCF 4.5 mm	292.7	295.8	Nabla	178	25
ZW 687a 15 kN	256.1	257.6	Skl 14	145	15
ZW 687a 20 kN	285.7	287.2	Skl 14	145	20
ZW 687a q	1 550.8	1 552.3	Skl 14	145	15

ERRI D 170/DT 283	RESULTS OF LINEAR COMPUTATIONS OF RELATIVE DISPLACEMENT BETWEEN RAIL AND SLEEPER (PART 1)	Tab. 2

Rail	Pad	Horizontal disp.		Vertical disp.		Rotation		Force in fastening		
		foot	head	ext.	int.	head	foot	Horiz.	Vert.	Mom.
		HP [mm]	HC[mm]	VPE[mm	VPI[mm]	RC[deg]	RP [deg]	Xy [kN]	Xz [kN]	X[kNm
Radius of curve 150 m										
Case nr.4 (cant deficiency 160 mm)										
1	Pandrol	-0.165	-3.380	-2.066	0.332	1.257	1.157	-41.25	44.75	1.93
	Pandrol. q	-0.167	-2.515	-1.275	0.290	0.918	0.763	-41.72	49.23	2.44
	ZW700	-0.404	-2.999	-1.510	0.302	1.015	0.880	-36.40	47.75	2.23
	SNCF 9mm	-0.406	-2.658	-1.201	0.275	0.880	0.721	-36.58	49.65	2.47
	SNCF 4.5mm	-0.231	-1.689	-0.490	0.159	0.570	0.331	-41.12	54.57	3.33
	ZW687a 15kN	-0.275	-1.806	-0.556	0.174	0.599	0.369	-39.92	54.09	3.21
	ZW687a 20kN	-0.276	-1.746	-0.503	0.161	0.575	0.339	-40.01	54.47	3.29
	ZW687a. q	-0.283	-1.251	-0.078	0.032	0.379	0.079	-41.00	57.60	4.14
2	Pandrol	0.252	4.447	-2.600	0.577	-1.641	-1.533	62.91	52.22	-2.56
	Pandrol. q	0.254	3.319	-1.617	0.488	-1.198	-1.017	63.57	57.46	-3.25
	ZW700	0.615	3.995	-1.908	0.498	-1.322	-1.168	55.32	55.72	-2.97
	SNCF 9mm	0.617	3.549	-1.523	0.442	-1.147	-0.959	55.57	57.94	-3.29
	SNCF 4.5mm	0.351	2.244	-0.629	0.242	-0.740	-0.445	62.48	63.70	-4.47
	ZW687a 15kN	0.418	2.407	-0.713	0.266	-0.778	-0.495	60.64	63.13	-4.31
	ZW687a 20kN	0.419	2.328	-0.645	0.246	-0.746	-0.454	60.76	63.57	-4.42
	ZW687a. q	0.429	1.672	-0.101	0.047	-0.486	-0.107	62.17	67.23	-5.60
Case nr.6 (cant excess 160 mm)										
1	Pandrol	-0.186	-4.983	-2.719	0.695	1.876	1.647	-46.51	52.24	2.75
	Pandrol. q	-0.189	-3.728	-1.681	0.531	1.384	1.079	-47.13	57.48	3.45
	ZW700	-0.460	-4.364	-1.992	0.581	1.527	1.249	-41.36	55.74	3.17
	SNCF 9mm	-0.462	-3.869	-1.586	0.505	1.333	1.021	-41.60	57.97	3.50
	SNCF 4.5mm	-0.262	-2.520	-0.646	0.260	0.883	0.463	-46.69	63.72	4.65
	ZW687a 15kN	-0.313	-2.677	-0.735	0.288	0.925	0.517	-45.37	63.16	4.50
	ZW687a 20kN	-0.314	-2.591	-0.664	0.265	0.891	0.474	-45.49	63.60	4.61
	ZW687a. q	-0.323	-1.884	-0.103	0.048	0.611	0.109	-46.77	67.26	5.74
2	Pandrol	0.201	2.678	-1.994	-0.031	-0.969	-0.948	50.24	52.25	-1.58
	Pandrol. q	0.203	2.003	-1.227	0.077	-0.704	-0.636	50.70	57.50	-2.03
	ZW700	0.488	2.470	-1.452	0.041	-0.775	-0.725	43.93	55.76	-1.84
	SNCF 9mm	0.490	2.203	-1.153	0.072	-0.670	-0.598	44.10	57.99	-2.05
	SNCF 4.5mm	0.279	1.368	-0.470	0.083	-0.426	-0.283	49.63	63.75	-2.84
	ZW687a 15kN	0.332	1.478	-0.534	0.087	-0.448	-0.314	48.14	63.18	-2.73
	ZW687a 20kN	0.333	1.429	-0.483	0.083	-0.429	-0.289	48.22	63.63	-2.81
	ZW687a. q	0.339	1.026	-0.075	0.020	-0.269	-0.069	49.21	67.29	-3.61

RC = (HP - HC)/146.5 mm * 180/pi

ERRI D 170/DT 283	RESULTS OF LINEAR COMPUTATIONS OF RELATIVE DISPLACEMENT BETWEEN RAIL AND SLEEPER (PART 2)	Tab. 3

Rail	Pad	Horizontal disp.		Vertical disp.		Rotation		Force in fastening		
		foot	head	ext.	int.	head	foot	Horiz.	Vert.	Mom.
		HP [mm]	HC[mm]	VPE[mm	VPI[mm]	RC[deg]	RP [deg]	Xy [kN]	Xz [kN]	X[kNm
Radius of curve >400 m										
Case nr.2 (cant deficiency 160 mm)										
1	Pandrol	-0.124	-2.465	-1.747	0.012	0.915	0.849	-31.05	44.76	1.42
	Pandrol. q	-0.126	-1.832	-1.067	0.082	0.667	0.560	-31.40	49.25	1.79
	ZW700	-0.304	-2.190	-1.270	0.061	0.737	0.646	-27.38	47.76	1.64
	SNCF 9mm	-0.306	-1.940	-1.005	0.079	0.639	0.529	-27.51	49.66	1.81
	SNCF 4.5mm	-0.174	-1.227	-0.404	0.073	0.412	0.243	-30.92	54.59	2.45
	ZW687a 15kN	-0.207	-1.314	-0.460	0.077	0.433	0.272	-30.02	54.10	2.36
	ZW687a 20kN	-0.207	-1.270	-0.415	0.073	0.415	0.249	-30.09	54.48	2.42
	ZW687a. q	-0.213	-0.907	-0.064	0.017	0.271	0.058	-30.82	57.61	3.05
2	Pandrol	0.197	3.227	-2.175	0.151	-1.185	-1.123	49.30	52.23	-1.87
	Pandrol. q	0.199	2.407	-1.340	0.190	-0.864	-0.746	49.80	57.47	-2.39
	ZW700	0.481	2.916	-1.587	0.176	-0.952	-0.856	43.29	55.73	-2.17
	SNCF 9mm	0.483	2.592	-1.261	0.180	-0.825	-0.704	43.47	57.96	-2.41
	SNCF 4.5mm	0.275	1.629	-0.514	0.128	-0.530	-0.328	48.89	63.72	-3.29
	ZW687a 15kN	0.327	1.751	-0.584	0.137	-0.557	-0.365	47.44	63.15	-3.17
	ZW687a 20kN	0.328	1.693	-0.528	0.129	-0.534	-0.335	47.54	63.59	-3.26
	ZW687a. q	0.335	1.214	-0.082	0.028	-0.344	-0.079	48.60	67.25	-4.14
Case nr.5 (cant excess 160 mm)										
1	Pandrol	-0.132	-3.763	-2.293	0.269	1.420	1.237	-32.90	52.25	2.07
	Pandrol. q	-0.133	-2.817	-1.404	0.254	1.049	0.808	-33.36	57.49	2.59
	ZW700	-0.326	-3.285	-1.671	0.260	1.157	0.937	-29.32	55.75	2.38
	SNCF 9mm	-0.328	-2.913	-1.324	0.243	1.011	0.765	-29.50	57.98	2.62
	SNCF 4.5mm	-0.186	-1.905	-0.532	0.145	0.672	0.346	-33.10	63.74	3.48
	ZW687a 15kN	-0.222	-2.021	-0.606	0.159	0.704	0.387	-32.17	63.18	3.37
	ZW687a 20kN	-0.222	-1.956	-0.547	0.148	0.678	0.354	-32.26	63.62	3.45
	ZW687a. q	-0.229	-1.425	-0.084	0.030	0.468	0.082	-33.20	67.29	4.28
2	Pandrol	0.144	1.913	-1.424	-0.022	-0.692	-0.677	35.89	37.32	-1.13
	Pandrol. q	0.145	1.431	-0.876	0.055	-0.503	-0.454	36.21	41.07	-1.45
	ZW700	0.349	1.764	-1.037	0.029	-0.554	-0.518	31.38	39.83	-1.31
	SNCF 9mm	0.350	1.573	-0.824	0.051	-0.478	-0.427	31.50	41.42	-1.46
	SNCF 4.5mm	0.199	0.977	-0.336	0.060	-0.304	-0.202	35.45	45.54	-2.03
	ZW687a 15kN	0.237	1.056	-0.381	0.062	-0.320	-0.224	34.38	45.13	-1.95
	ZW687a 20kN	0.238	1.021	-0.345	0.060	-0.306	-0.206	34.45	45.45	-2.01
	ZW687a. q	0.242	0.733	-0.053	0.015	-0.192	-0.049	35.15	48.06	-2.58

RC = (HP - HC)/146.5 mm * 180/pi

ERRI D 170/DT 283	RESULTS OF NON-LINEAR COMPUTATIONS OF RELATIVE DISPLACEMENT BETWEEN RAIL AND SLEEPER (PART 1)	Tab. 4

Rail	Pad	Horizontal disp.		Vertical disp.		Rotation		Force in fastening		
		foot	head	ext.	int.	head	foot	Horiz.	Vert.	Mom.
		HP [mm]	HC[mm]	VPE[mm	VPI[mm]	RC[deg]	RP [deg]	Xy [kN]	Xz [kN]	X[kNm
Radius of curve 150 m										
Case nr.4 (cant deficiency 160 mm)										
1	Pandrol	-0.167	-3.354	-1.922	0.365	1.246	1.108	-41.74	50.03	2.39
	Pandrol. q	-0.172	-2.240	-0.845	0.310	0.809	0.573	-42.96	57.87	3.33
	ZW700	-0.408	-2.783	-1.368	0.202	0.929	0.766	-36.70	49.85	2.53
	SNCF 9mm	-0.414	-2.383	-0.879	0.237	0.770	0.553	-37.23	55.56	3.10
	SNCF 4.5mm	-0.233	-1.653	-0.361	0.211	0.555	0.296	-41.41	57.99	3.53
	ZW687a 15kN	-0.276	-1.821	-0.443	0.274	0.604	0.364	-40.07	58.01	3.32
	ZW687a 20kN	-0.277	-1.760	-0.407	0.243	0.580	0.332	-40.16	57.65	3.40
	ZW687a. q	-0.277	-1.480	-0.153	0.239	0.470	0.210	-40.16	59.57	3.51
2	Pandrol	0.253	4.401	-2.308	0.744	-1.622	-1.477	63.27	58.62	-3.00
	Pandrol. q	0.261	2.880	-0.903	0.573	-1.025	-0.734	65.17	70.09	-4.43
	ZW700	0.619	3.634	-1.647	0.364	-1.179	-0.982	55.75	58.88	-3.41
	SNCF 9mm	0.627	3.107	-0.998	0.418	-0.970	-0.703	56.43	66.36	-4.15
	SNCF 4.5mm	0.352	2.210	-0.428	0.369	-0.727	-0.411	62.72	69.19	-4.64
	ZW687a 15kN	0.418	2.494	-0.538	0.517	-0.812	-0.531	60.56	69.90	-4.25
	ZW687a 20kN	0.419	2.365	-0.494	0.412	-0.761	-0.462	60.81	68.71	-4.46
	ZW687a. q	0.419	2.094	-0.216	0.451	-0.655	-0.347	60.74	71.54	-4.50
Case nr.6 (cant excess 160 mm)										
1	Pandrol	-0.187	-5.046	-2.407	0.982	1.900	1.638	-46.83	57.96	3.16
	Pandrol. q	-0.195	-3.334	-0.911	0.727	1.228	0.812	-48.69	69.76	4.63
	ZW700	-0.464	-3.955	-1.700	0.439	1.365	1.044	-41.76	59.21	3.61
	SNCF 9mm	-0.472	-3.403	-1.019	0.496	1.146	0.752	-42.47	65.98	4.38
	SNCF 4.5mm	-0.264	-2.507	-0.438	0.413	0.878	0.438	-46.91	69.00	4.81
	ZW687a 15kN	-0.312	-2.867	-0.558	0.635	0.999	0.598	-45.28	69.94	4.39
	ZW687a 20kN	-0.314	-2.663	-0.508	0.466	0.919	0.495	-45.54	68.57	4.64
	ZW687a. q	-0.313	-2.408	-0.228	0.527	0.819	0.391	-45.46	71.51	4.65
2	Pandrol	0.203	2.412	-1.829	-0.198	-0.864	-0.793	50.87	58.51	-2.14
	Pandrol. q	0.208	1.607	-0.833	-0.045	-0.547	-0.395	52.00	65.87	-2.96
	ZW700	0.491	2.342	-1.331	0.002	-0.724	-0.650	44.22	58.18	-2.10
	SNCF 9mm	0.498	1.905	-0.851	-0.011	-0.550	-0.419	44.80	64.07	-2.72
	SNCF 4.5mm	0.281	1.282	-0.342	0.082	-0.391	-0.223	50.02	66.88	-3.12
	ZW687a 15kN	0.334	1.406	-0.417	0.090	-0.419	-0.262	48.48	66.32	-2.99
	ZW687a 20kN	0.335	1.376	-0.383	0.094	-0.407	-0.247	48.51	66.32	-3.02
	ZW687a. q	0.336	1.146	-0.132	0.112	-0.317	-0.138	48.69	67.63	-3.23

RC = (HP - HC)/146.5 mm * 180/pi

ERRI D 170/DT 283	RESULTS OF NON-LINEAR COMPUTATIONS OF RELATIVE DISPLACEMENT BETWEEN RAIL AND SLEEPER (PART 2)	Tab. 5

Rail	Pad	Horizontal disp.		Vertical disp.		Rotation		Force in fastening		
		foot	head	ext.	int.	head	foot	Horiz.	Vert.	Mom.
		HP [mm]	HC[mm]	VPE[mm	VPI[mm]	RC[deg]	RP [deg]	Xy [kN]	Xz [kN]	X[kNm
Radius of curve >400 m										
Case nr.2 (cant deficiency 160 mm)										
1	Pandrol	-0.127	-2.332	-1.685	-0.132	0.863	0.754	-31.63	49.49	1.91
	Pandrol. q	-0.130	-1.581	-0.807	-0.011	0.568	0.396	-32.40	55.33	2.51
	ZW700	-0.307	-2.098	-1.198	0.016	0.701	0.591	-27.60	49.45	1.84
	SNCF 9mm	-0.312	-1.735	-0.800	0.005	0.556	0.400	-28.06	54.08	2.34
	SNCF 4.5mm	-0.175	-1.175	-0.316	0.071	0.391	0.202	-31.24	56.83	2.67
	ZW687a 15kN	-0.209	-1.276	-0.381	0.081	0.417	0.237	-30.29	56.39	2.57
	ZW687a 20kN	-0.209	-1.246	-0.348	0.084	0.406	0.223	-30.32	56.43	2.59
	ZW687a. q	-0.210	-1.006	-0.110	0.088	0.311	0.112	-30.45	57.81	2.77
2	Pandrol	0.200	3.011	-1.966	0.072	-1.100	-0.989	49.88	58.42	-2.42
	Pandrol. q	0.205	1.982	-0.854	0.114	-0.695	-0.484	51.22	66.91	-3.41
	ZW700	0.485	2.713	-1.424	0.102	-0.872	-0.745	43.63	58.22	-2.50
	SNCF 9mm	0.491	2.249	-0.894	0.111	-0.687	-0.500	44.22	64.68	-3.14
	SNCF 4.5mm	0.277	1.543	-0.367	0.150	-0.495	-0.270	49.28	67.19	-3.58
	ZW687a 15kN	0.329	1.698	-0.448	0.183	-0.535	-0.323	47.73	66.99	-3.39
	ZW687a 20kN	0.330	1.656	-0.413	0.172	-0.519	-0.302	47.78	66.79	-3.45
	ZW687a. q	0.330	1.390	-0.153	0.177	-0.415	-0.181	47.89	68.35	-3.61
Case nr.5 (cant excess 160 mm)										
1	Pandrol	-0.134	-3.606	-2.056	0.272	1.358	1.128	-33.41	57.69	2.60
	Pandrol. q	-0.139	-2.391	-0.864	0.225	0.881	0.543	-34.76	66.54	3.63
	ZW700	-0.330	-3.013	-1.476	0.156	1.050	0.797	-29.66	59.34	2.72
	SNCF 9mm	-0.336	-2.531	-0.915	0.182	0.859	0.546	-30.22	64.59	3.35
	SNCF 4.5mm	-0.188	-1.831	-0.376	0.179	0.642	0.289	-33.48	67.09	3.75
	ZW687a 15kN	-0.224	-1.990	-0.464	0.239	0.691	0.359	-32.42	66.91	3.56
	ZW687a 20kN	-0.224	-1.934	-0.426	0.211	0.669	0.327	-32.49	66.74	3.62
	ZW687a. q	-0.224	-1.642	-0.161	0.207	0.554	0.200	-32.52	68.57	3.74
2	Pandrol	0.146	1.882	-1.500	-0.196	-0.679	-0.633	36.39	40.87	-1.51
	Pandrol. q	0.148	1.305	-0.765	-0.035	-0.453	-0.361	36.91	45.49	-1.93
	ZW700	0.351	1.744	-1.025	-0.001	-0.545	-0.498	31.55	40.71	-1.44
	SNCF 9mm	0.354	1.465	-0.731	-0.020	-0.435	-0.351	31.90	44.33	-1.83
	SNCF 4.5mm	0.200	0.952	-0.286	0.056	-0.294	-0.177	35.68	47.24	-2.18
	ZW687a 15kN	0.238	1.039	-0.340	0.060	-0.313	-0.204	34.58	46.88	-2.09
	ZW687a 20kN	0.239	1.012	-0.307	0.065	-0.302	-0.191	34.60	46.94	-2.11
	ZW687a. q	0.240	0.805	-0.089	0.067	-0.221	-0.090	34.83	48.12	-2.35

RC = (HP - HC)/146.5 mm * 180/pi

ERRI D 170/DT 283	DIFFERENCES BETWEEN LINEAR AND NON-LINEAR COMPUTATION RESULTS OF RELATIVE DISPLACEMENT BETWEEN RAIL AND SLEEPER (PART 1)	Tab. 6

Rail	Pad	Horizontal disp.		Vertical disp.		Rotation		Force in fastening		
		foot	head	ext.	int.	head	foot	Horiz.	Vert.	Mom.
		HP [mm]	HC[mm]	VPE[mm	VPI[mm]	RC[deg]	RP [deg]	Xy [kN]	Xz [kN]	X[kNm
Radius of curve 150 m										
Case nr.4 (cant deficiency 160 mm)										
1	Pandrol	1.2	-0.8	-7.0	9.9	-0.9	-4.2	1.2	11.8	23.8
	Pandrol. q	3.0	-10.9	-33.7	6.9	-11.9	-24.9	3.0	17.6	36.5
	ZW700	1.0	-7.2	-9.4	-33.1	-8.5	-13.0	0.8	4.4	13.5
	SNCF 9mm	2.0	-10.3	-26.8	-13.8	-12.5	-23.3	1.8	11.9	25.5
	SNCF 4.5mm	0.9	-2.1	-26.3	32.7	-2.6	-10.6	0.7	6.3	6.0
	ZW687a 15kN	0.4	0.8	-20.3	57.5	0.8	-1.4	0.4	7.2	3.4
	ZW687a 20kN	0.4	0.8	-19.1	50.9	0.9	-2.1	0.4	5.8	3.3
	ZW687a. q	-2.1	18.3	96.2	646.9	24.0	165.8	-2.0	3.4	-15.2
2	Pandrol	0.4	-1.0	-11.2	28.9	-1.2	-3.7	0.6	12.3	17.2
	Pandrol. q	2.8	-13.2	-44.2	22.4	-14.4	-27.8	2.5	22.0	36.3
	ZW700	0.7	-9.0	-13.7	-26.9	-10.8	-15.9	0.8	5.7	14.8
	SNCF 9mm	1.6	-12.5	-34.5	-5.4	-15.4	-26.7	1.5	14.5	26.1
	SNCF 4.5mm	0.3	-1.5	-32.0	52.5	-1.8	-7.6	0.4	8.6	3.8
	ZW687a 15kN	0.0	3.6	-24.5	94.4	4.4	7.3	-0.1	10.7	-1.4
	ZW687a 20kN	0.0	1.6	-23.4	67.5	2.0	1.8	0.1	8.1	0.9
	ZW687a. q	-2.3	25.2	113.9	859.6	34.8	224.3	-2.3	6.4	-19.6
Case nr.6 (cant excess 160 mm)										
1	Pandrol	0.5	1.3	-11.5	41.3	1.3	-0.5	0.7	10.9	14.9
	Pandrol. q	3.2	-10.6	-45.8	36.9	-11.3	-24.7	3.3	21.4	34.2
	ZW700	0.9	-9.4	-14.7	-24.4	-10.6	-16.4	1.0	6.2	13.9
	SNCF 9mm	2.2	-12.0	-35.8	-1.8	-14.0	-26.3	2.1	13.8	25.1
	SNCF 4.5mm	0.8	-0.5	-32.2	58.8	-0.6	-5.4	0.5	8.3	3.4
	ZW687a 15kN	-0.3	7.1	-24.1	120.5	8.0	15.7	-0.2	10.7	-2.4
	ZW687a 20kN	0.0	2.8	-23.5	75.8	3.1	4.4	0.1	7.8	0.7
	ZW687a. q	-3.1	27.8	121.4	997.9	34.0	258.7	-2.8	6.3	-19.0
2	Pandrol	1.0	-9.9	-8.3	538.7	-10.8	-16.4	1.3	12.0	35.4
	Pandrol. q	2.5	-19.8	-32.1	-158.4	-22.3	-37.9	2.6	14.6	45.8
	ZW700	0.6	-5.2	-8.3	-95.1	-6.6	-10.3	0.7	4.3	14.1
	SNCF 9mm	1.6	-13.5	-26.2	-115.3	-17.9	-29.9	1.6	10.5	32.7
	SNCF 4.5mm	0.7	-6.3	-27.2	-1.2	-8.2	-21.2	0.8	4.9	9.9
	ZW687a 15kN	0.6	-4.9	-21.9	3.4	-6.5	-16.6	0.7	5.0	9.5
	ZW687a 20kN	0.6	-3.7	-20.7	13.3	-5.1	-14.5	0.6	4.2	7.5
	ZW687a. q	-0.9	11.7	76.0	460.0	17.8	100.0	-1.1	0.5	-10.5

VALUES IN %

ERRI D 170/DT 283	DIFFERENCES BETWEEN LINEAR AND NON-LINEAR COMPUTATION RESULTS OF RELATIVE DISPLACEMENT BETWEEN RAIL AND SLEEPER (PART 2)	Tab. 7

Rail	Pad	Horizontal disp.		Vertical disp.		Rotation		Force in fastening		
		foot	head	ext.	int.	head	foot	Horiz.	Vert.	Mom.
		HP [mm]	HC[mm]	VPE[mm	VPI[mm]	RC[deg]	RP [deg]	Xy [kN]	Xz [kN]	X[kNm
Radius of curve >400 m										
Case nr.2 (cant deficiency 160 mm)										
1	Pandrol	2.4	-5.4	-3.5	-1200.0	-5.7	-11.2	1.9	10.6	34.5
	Pandrol. q	3.2	-13.7	-24.4	-113.4	-14.8	-29.3	3.2	12.3	40.2
	ZW700	1.0	-4.2	-5.7	-73.8	-4.9	-8.5	0.8	3.5	12.2
	SNCF 9mm	2.0	-10.6	-20.4	-93.7	-13.0	-24.4	2.0	8.9	29.3
	SNCF 4.5mm	0.6	-4.2	-21.8	-2.7	-5.1	-16.9	1.0	4.1	9.0
	ZW687a 15kN	1.0	-2.9	-17.2	5.2	-3.7	-12.9	0.9	4.2	8.9
	ZW687a 20kN	1.0	-1.9	-16.1	15.1	-2.2	-10.4	0.8	3.6	7.0
	ZW687a. q	-1.4	10.9	71.9	417.6	14.8	93.1	-1.2	0.3	-9.2
2	Pandrol	1.5	-6.7	-9.6	-52.3	-7.2	-11.9	1.2	11.9	29.4
	Pandrol. q	3.0	-17.7	-36.3	-40.0	-19.6	-35.1	2.9	16.4	42.7
	ZW700	0.8	-7.0	-10.3	-42.0	-8.4	-13.0	0.8	4.5	15.2
	SNCF 9mm	1.7	-13.2	-29.1	-38.3	-16.7	-29.0	1.7	11.6	30.3
	SNCF 4.5mm	0.7	-5.3	-28.6	17.2	-6.6	-17.7	0.8	5.4	8.8
	ZW687a 15kN	0.6	-3.0	-23.3	33.6	-3.9	-11.5	0.6	6.1	6.9
	ZW687a 20kN	0.6	-2.2	-21.8	33.3	-2.8	-9.9	0.5	5.0	5.8
	ZW687a. q	-1.5	14.5	86.6	532.1	20.6	129.1	-1.5	1.6	-12.8
Case nr.5 (cant excess 160 mm)										
1	Pandrol	1.5	-4.2	-10.3	1.1	-4.4	-8.8	1.6	10.4	25.6
	Pandrol. q	4.5	-15.1	-38.5	-11.4	-16.0	-32.8	4.2	15.7	40.2
	ZW700	1.2	-8.3	-11.7	-40.0	-9.2	-14.9	1.2	4.6	14.3
	SNCF 9mm	2.4	-13.1	-30.9	-25.1	-15.0	-28.6	2.4	11.4	27.9
	SNCF 4.5mm	1.1	-3.9	-29.3	23.4	-4.5	-16.5	1.1	5.3	7.8
	ZW687a 15kN	0.9	-1.5	-23.4	50.3	-1.8	-7.2	0.8	5.9	5.6
	ZW687a 20kN	0.9	-1.1	-22.1	42.6	-1.3	-7.6	0.7	4.9	4.9
	ZW687a. q	-2.2	15.2	91.7	590.0	18.4	143.9	-2.0	1.9	-12.6
2	Pandrol	1.4	-1.6	5.3	790.9	-1.9	-6.5	1.4	9.5	33.6
	Pandrol. q	2.1	-8.8	-12.7	-163.6	-9.9	-20.5	1.9	10.8	33.1
	ZW700	0.6	-1.1	-1.2	-103.4	-1.6	-3.9	0.5	2.2	9.9
	SNCF 9mm	1.1	-6.9	-11.3	-139.2	-9.0	-17.8	1.3	7.0	25.3
	SNCF 4.5mm	0.5	-2.6	-14.9	-6.7	-3.3	-12.4	0.6	3.7	7.4
	ZW687a 15kN	0.4	-1.6	-10.8	-3.2	-2.2	-8.9	0.6	3.9	7.2
	ZW687a 20kN	0.4	-0.9	-11.0	8.3	-1.3	-7.3	0.4	3.3	5.0
	ZW687a. q	-0.8	9.8	67.9	346.7	15.1	83.7	-0.9	0.1	-8.9

VALUES IN %

ERRI D 170/DT 283	DISTRIBUTION COEFFICIENTS FOR SLEEPER LOADING COMPUTED FROM EQUATION (32)	Tab. 8

Linear distribution coefficient

Case	Rail	Pandrol	SNCF 9 mm	SNCF 4.5	ZW687a
All	Both	0.373	0.414	0.455	0.451

Non-linear distribution coefficient

Case	Rail	Pandrol	SNCF 9 mm	SNCF 4.5	ZW687a
2	1	0.4125	0.451	0.474	0.470
	2	0.417	0.462	0.436	0.480
4	1	0.417	0.463	0.483	0.484
	2	0.419	0.474	0.494	0.500
5	1	0.412	0.461	0.479	0.478
	2	0.408	0.443	0.472	0.469
6	1	0.414	0.471	0.492	0.500
	2	0.418	0.458	0.478	0.474